DISSERTATIONES
CHIMICAE
UNIVERSITATIS
TARTUENSIS
214

MARIS-JOHANNA TAHK

Novel fluorescence-based methods for illuminating transmembrane signal transduction by G-protein coupled receptors

DISSERTATIONES CHIMICAE UNIVERSITATIS TARTUENSIS
214

DISSERTATIONES CHIMICAE UNIVERSITATIS TARTUENSIS
214

MARIS-JOHANNA TAHK

Novel fluorescence-based methods for illuminating transmembrane signal transduction by G-protein coupled receptors

UNIVERSITY OF TARTU
Press
1632

Institute of Chemistry, Faculty of Science and Technology, University of Tartu, Estonia

The dissertation is accepted for the commencement of the degree of Doctor of Philosophy in Chemistry on June 17th, 2022, by the Council of Institute of Chemistry, University of Tartu.

Supervisor: Professor Ago Rinken
Institute of Chemistry, University of Tartu, Estonia

Opponent: Dr. Isabel D. Alves
CNSA, University of Bordeaux, France

Commencement: 24.08.2022, at 12:15. Auditorium 1020, Ravila 14a, Tartu

This work was supported by the Estonian Ministry of Education and Science (IUT 20-17 and PSG230) and the University of Tartu ASTRA Project PER ASPERA, NATO (SPS 985261) and the European Union through the European Regional Development Fund (EU48695) and by the Enterprise Estonia Applied research programme 2021. and by COST action CA18133 ERNEST.

This work has been supported by the Graduate School of Functional materials and technologies, receiving funding from the European Regional Development Fund in the University of Tartu, Estonia

ISSN 1406-0299
ISBN 978-9949-03-935-7 (print)
ISBN 978-9949-03-936-4 (pdf)

University of Tartu Press
www.tyk.ee

CONTENTS

LIST OF ORIGINAL PUBLICATIONS

The current thesis is based on the following original publications, referred to in the text by corresponding Roman numerals:

I. Veiksina, S., **M.-J. Tahk**, T. Laasfeld, R. Link, S. Kopanchuk and A. Rinken (2021). Fluorescence Anisotropy-Based Assay for Characterization of Ligand Binding Dynamics to GPCRs: The Case of Cy3B-Labeled Ligands Binding to MC_4 Receptors in Budded Baculoviruses. In: Martins S.A.M., Prazeres D.M.F. (eds) G Protein-Coupled Receptor Screening Assays. Methods in Molecular Biology, vol 2268. Humana, New York, NY. https://doi.org/10.1007/978-1-0716-1221-7_8

II. Lavogina, D., T. Laasfeld, **M.-J. Tahk**, O. Kukk, A. Allikalt, S. Kopanchuk and A. Rinken (2021). cAMP Biosensor Assay Using BacMam Expression System: Studying the Downstream Signaling of LH/hCG Receptor Activation. In: Martins S.A.M., Prazeres D.M.F. (eds) G Protein-Coupled Receptor Screening Assays. Methods in Molecular Biology, vol 2268. Humana, New York, NY. https://doi.org/10.1007/978-1-0716-1221-7_12

III. Link, R., S. Veiksina, **M.- J. Tahk,** T. Laasfeld, P. Paiste, S. Kopanchuk, & A. Rinken. (2020). The constitutive activity of melanocortin-4 receptors in cAMP pathway is allosterically modulated by zinc and copper ions. Journal of Neurochemistry. 153:346–361. https://doi.org/10.1111/jnc.14933

IV. Müller C., J. Gleixner, **M.-J. Tahk**, S. Kopanchuk, T. Laasfeld, M. Weinhart, D. Schollmeyer, M. U. Betschart, S. Lüdeke, P. Koch, A. Rinken and M. Keller (2022). Structure-Based Design of High-Affinity Fluorescent Probes for the Neuropeptide Y Y1 Receptor. Journal of Medicinal Chemistry 65 (6), 4832–4853 https://doi.org/10.1021/acs.jmedchem.1c02033

V. Laasfeld, T., R. Ehrminger, **M.- J. Tahk**, S. Veiksina, K. R. Kolvart, M. Min, S. Kopanchuk and A. Rinken (2021). Budded baculoviruses as a receptor display system to quantify ligand binding with TIRF microscopy. *Nanoscale*, 13, 2436–2447. https://doi.org/10.1039/D0NR06737G

VI. Grätz, L., T. Laasfeld, A. Allikalt, C. G. Gruber, A. Pegoli, **M.-J. Tahk**, M.-L. Tsernant, M. Keller and A. Rinken (2021). BRET- and fluorescence anisotropy-based assays for real-time monitoring of ligand binding to M2 muscarinic acetylcholine receptors, Biochimica et Biophysica Acta (BBA) – Molecular Cell Research, 1868(3), 118930, https://doi.org/10.1016/j.bbamcr.2020.118930

VII. **Tahk, M.- J.**, J. Torp, M. A. S. Ali, D. Fishman, L. Parts, L. Grätz, C. Müller, M. Keller, S. Veiksina, T. Laasfeld and A. Rinken (2022). Live-cell microscopy or fluorescence anisotropy with budded baculoviruses – which way to go with measuring ligand binding to M4 muscarinic receptors? *Open Biology, 12*(6), 220019, https://doi.org/10.1098/rsob.220019

Author's contribution:

I. The author participated in the formulation of protocol and the writing of the article.

II. The author cloned the biosensor into the BacMam system, produced the virus, made the initial assay optimisation and participated in writing the article.

III. The author developed and optimised the assay for cAMP detection and performed some experiments and data analysis for the cAMP detection.

IV. The author prepared the BBV particles, performed the fluorescence anisotropy and microscopy experiments, and participated in writing the corresponding parts of the manuscript.

V. The author performed fluorescence anisotropy experiments and data analysis and wrote the manuscript.

VI. The author prepared the BBV particles and supervised the fluorescence anisotropy experiments.

VII. The author was the principal investigator responsible for planning and performing the experiments, data analysis, and writing the manuscript.

ABBREVIATIONS

AB	assay buffer
ATP	adenosine triphosphate
BacMam	a recombinant baculovirus for delivering genes of interest into mammalian cells
Bacmid	baculovirus shuttle vector
BBV	budded baculovirus
BV	baculoviruses
BRET	bioluminescence resonance energy transfer
cAMP	3',5'-cyclic adenosine monophosphate
DPBS	Dulbecco's Phosphate-Buffered Saline
DMEM	Dulbecco's Modified Eagle's Medium
EC_{50}	concentration of the sample that produces 50% of the maximal possible effect
FA	fluorescence anisotropy
FRET	Förster/fluorescence resonance energy transfer
GTP	Guanosine triphosphate
GPCR	G-protein coupled receptors
HTS	high throughput screening
IC_{50}	molar concentration of ligand that inhibits binding of a labelled ligand by 50%
IP_3	inositol 1,4,5-triphosphate
ivp	infectious viral particles
K_D	equilibrium dissociation constant of a ligand determined directly in a binding assay using a labelled ligand
K_i	inhibition constant refers to an equilibrium dissociation constant of an unlabelled ligand measured in competition with a labelled ligand
k_{off}	dissociation rate constant
k_{on}	association rate constant
MOI	multiplicity of infection
NPY	neuropeptide Y
Sf9	*Spodoptera frugiperda* cells
SEM	standard error of the mean
TFI	total fluorescence intensity
TRIS	2-Amino-2-(hydroxymethyl)propane-1,3-diol

INTRODUCTION

For an organism to survive and even thrive in an environment, it needs to understand and respond to the changes in the environment. Furthermore, to have cooperation between smaller units like cells, they need to exchange information. On a larger scale, humans have eyes, nose, ears and skin to receive information, on a smaller scale, cells have receptors. Being one of the largest receptor classes, G-protein coupled receptors are also ubiquitously expressed in the human body. However, abnormalities in the signalling processes lead to diseases, making G-protein coupled receptors attractive drug targets. The drug discovery process ranges from identifying the target and synthesising new molecules to evaluating pharmacological properties and clinical trials. The mode of action of a new drug is complicated, and therefore many different assays are needed to obtain a comprehensive profile.

Although G-protein coupled receptors can be found in the whole human body, the average concentrations are so small that they can not be characterized with ordinary biochemical methods. Using radioligands with suitable methods has been a gold standard in this field until the last decade. However, the development of fluorescence technologies has opened a new era in receptor research. Still, fluorescence approaches are neither simple nor straightforward. Furthermore, all new methods need to be validated and compared to a standard. Thus the aim of this thesis was to find new possibilities to study ligand binding properties for different GPCRs. In addition, the results from different assays for the same receptors were compared and pooled to obtain a more comprehensive understanding of receptor-ligand interactions and modulation.

1. LITERATURE OVERVIEW

1.1. G-protein coupled receptors

Cells are the building blocks of higher lifeforms. However, for cells to cooperate, they need to receive, process, and send information. Information in nature takes many forms, from molecules and ions like the small hydrogen ion to temperature, pressure, and light. These signals are transduced through the membrane by proteins called receptors. The signalling molecules which bind to the receptor are called ligands. Receptors transmit the signal from outside the cell to the inside the cell via a series of molecular events. Receptors have been broadly classified into six basic classes: G-protein coupled receptors (GPCRs), receptor tyrosine kinases, receptor guanylyl cyclases, gated ion channels, adhesion receptors and intracellular nuclear receptors (Nelson *et al.* 2008).

GPCRs are the most prominent family of membrane receptors, with 800 different receptors identified in humans (Bjarnadóttir *et al.* 2006). All of these have the same structural elements: an extracellular N-terminus, an intracellular C-terminus and seven transmembrane α-helices connected by three intracellular and three extracellular loops (Palczewski *et al.* 2000). The extracellular domain where the ligand binds is the least conserved. In contrast, GPCRs have remarkable homology at the cytoplasmic ends of the transmembrane helices, indicating a conserved activation and signal transduction mechanism. GPCRs have been classified in many different ways, but based on the phylogenetic analyses, the "GRAFS" classification scheme divides vertebrate GPCRs into five classes: Rhodopsin, Secretin, Glutamate, Adhesion and Frizzled/Taste2 (Schiöth and Fredriksson 2005). (Mirzadegan *et al.* 2003)

GPCRs got their name after the heterotrimeric G proteins, which couple to the receptors from the intracellular side and may initiate many different intracellular signalling pathways. Heterotrimeric G protein complexes contain α, β and γ subunits. G stands for guanine nucleotide, which binds the α subunit of the heterotrimer. Humans have evolved a large variety of G proteins, encoding 18 different G_{α} proteins, 5 G_{β} proteins, and 12 G_{γ} proteins (Syrovatkina *et al.* 2016).

The conformational change of GPCR initiated by agonist binding causes the receptor coupled G proteins to activate. The conformational change of GPCRs catalyses the exchange of guanosine diphosphate (GDP) for guanosine tri-phosphate (GTP) in the α-subunit. GTP binding causes the G protein to dissociate from the receptor, yielding a monomeric α-subunit and a βγ dimer. Both of these can serve as activators of particular signalling pathway effectors. Depending on the α-subunits structure, it activates ($G_{\alpha s}$) or inhibits ($G_{\alpha i}$) adenylyl cyclase, increases the concentration of adenosine triphosphate (ATP) ($G_{\alpha 12/13}$) or modulates the levels of diacylglycerol, inositol 1,4,5-triphosphate (IP_3) and Ca^{2+} ions in the cell ($G_{\alpha q/11}$). Meanwhile, the $G_{\beta\gamma}$ dimer can recruit GPCR kinases to the membrane and regulate G-protein coupled, inwardly rectifying potassium channels, voltage-dependent Ca^{2+} channels, adenylyl cyclases, phospholipase C, phosphoinositide 3-kinase and mitogen-activated protein kinases (Hilger *et al.*

2018). The understanding of GPCR and G protein coupling profiles remains incomplete despite extensive studies in this field. Although GPCRs generally have a preference for specific G protein subtypes, it is common that they can couple also with G proteins from two or three different families. However, coupling to all four G protein families is rare (Hauser *et al.* 2022).

Besides G-protein signalling, GPCRs can also signal via β-arrestins. At first, β-arrestins were thought just to block the activated GPCRs. However, now it is known that they also trigger endocytosis and kinase activation leading to specific signalling pathways that can be localised on endosomes. These signalling pathways are also found to be independent of G protein activation by GPCRs. (Jean-Charles *et al.* 2017)

Information can arrive in many different forms, ranging from photons, tastants and odorants to ions, neurotransmitters, hormones, and cytokines (Wacker *et al.* 2017). The ligands that the organism synthesises are called endogenous ligands, such as acetylcholine and neuropeptide Y. The endogenous ligands have not been yet discovered for all GPCRs. The receptors for which endogenous ligand is not yet known are called orphan receptors. In 2005 there were over 140 orphan receptors (Levoye *et al.* 2006).

The site that binds the endogenous ligand is called the orthosteric site. The same endogenous ligand can bind to multiple receptors and receptor subtypes, thus, the orthosteric binding sites are structurally similar. However, there are also allosteric sites that are topographically distinct from the orthosteric site. GPCRs can have multiple allosteric sites but at least one allosteric site where the G protein binds. (Christopoulos and Kenakin 2002)

Ligands can be classified by origin into synthetic and natural substances or by biological activity as agonists, inverse agonists and antagonists. Agonists activate the receptor, which in turn initiates the intracellular signalling cascade leading to changes inside the cell. Not all agonists are equal, some agonists, called partial agonists, have smaller maximal biological responses than the endogenous agonist. Furthermore, a growing number of articles have been published about the concept of biased agonism – ligand-dependent activation of specific pathways over others. For example, mediating the G protein signal over the β-arrestin signal. Evidence shows that a biased agonist could reduce the amount and severity of drug side effects. This is based on the idea that the therapeutic effect is mediated by one pathway and the side effects by another. (Kolb *et al.* 2022)

One of the main categories of ligands are antagonists, which bind to the receptor's orthosteric site blocking the binding of any other orthosteric ligand but not activating the receptor. Lastly, the inverse agonists reduce the receptor's activity below the basal level (Neubig *et al.* 2003). This is possible because some receptors can be activated in an agonist-independent manner – the constitutive activity. Inverse agonism is a rare property because, in nature, only a few inverse agonists have been identified (de Ligt *et al.* 2000).

Because GPCRs are expressed throughout the human body, they have fundamental roles in virtually all physiological functions (Wacker *et al.* 2017). Moreover, problems with GPCR mediated signal transduction can also cause

various disorders, like allergies, depression, blindness, diabetes and various cardiovascular defects (Nelson *et al.* 2008). The estimated number of approved drugs that target GPCRs in 2017 was between 475 and 704, which makes up approximately 34% of approved drugs (Sriram and Insel 2018; Hauser *et al.* 2017). Widely used therapeutics targeting GPCRs include opioid analgesics, antihistamines, anticholinergics, antipsychotics, antimigraine drugs, and asthma drugs (Wacker *et al.* 2017). Furthermore, in 2017 only 134 of the 800 GPCRs were targets for drugs approved in the United States or European Union (Sriram and Insel 2018). Therefore, much work is still needed to find suitable drugs for most GPCRs. The first step in finding these ligands is developing an assay that can measure the many aspects of the interactions between the ligand and a specific receptor.

1.2. Ligand binding methods

At the beginning of experimental pharmacology, experiments were carried out on live animals or animal tissues. For example, muscarine as an active pharmacological substance was found by O.Schmiedeberg and R.Koppe in 1869 in Tartu. Following the extraction of muscarine, it was tested on dogs (Schmiedeberg 1869). Later, in 1876, Langley studied the effect of other ligands of muscarinic acetylcholine receptors in a more specific manner on salivary secretion in dogs. These experiments demonstrated that agonist pilocarpine stimulated salivary production, and antagonist atropine stopped it (Langley 1876). In this period, similar tissue responses were used as an assay readout to study the effects of the various chemicals.

The experiments with live animals, whole organs and later with bacteria led to the idea of a "receptive substance" on reactive cells in the first decade of the 20th century (Lefkowitz 2004). However, the discovery of radioactivity and the development of ligands labelled with radioactive isotopes changed the landscape of receptor research. Direct ligand binding assays allowed to obtain more knowledge about the interaction between a receptor and its ligands. The next step in direct ligand binding assay evolution was the development of fluorescent ligands, which are larger than radioligands but safer to use. Fluorescent ligands are used in many assay types, from high throughput screening (HTS) set-ups with plate readers to microscopy techniques that can detect single molecules. More and more creative ways of studying GPCR using fluorescent ligands are still being developed.

The receptor can be studied at different levels. The most direct method is monitoring ligand binding (radioligand binding assay, fluorescence anisotropy (FA)) or conformational changes in receptors' structure upon ligand binding (Förster resonance energy transfer (FRET)). The next level is studying the G protein activation by measuring GTPγS binding. One more level further from the receptor is the measurement of the second messengers like cAMP, IP_3 or Ca^{2+}, which can be easily done in live cells with biosensors. Lastly, the reporter gene

assays measure changes in gene expression, through the expression of a reporter gene, like luciferase, after the receptor activation. (Zhang and Xie 2012)

Different parameters can be obtained from ligand binding assays based on the assay set-up and method used. Kinetic parameters describe how fast the ligand binds to the receptor (k_{on}) or dissociates from the receptor (k_{off}). The dissociation constant K is numerically equal to the ratio of dissociation to association rate constants (k_{off} / k_{on}) and describes the affinity of the ligand to the specific receptor. However, different types of dissociation constants are derived from the experimental set-up. K_d refers to the equilibrium dissociation constant of a labelled ligand determined directly in a binding assay. In comparison, K_i refers to the equilibrium dissociation constant of an unlabeled ligand determined indirectly in a competition binding assay. As this is an indirect method, the affinity of the labelled ligand has to be previously determined. Classically, the Cheng–Prusoff formula is used to calculate the K_i values. However, this equation has several assumptions, like the labelled ligand concentration staying constant, that need to be considered before using it. Another frequently used parameter describes the about of receptor, usually defined by the maximal specific binding of a ligand (B_{max}, R_{stock}). The ligand-receptor complex formation can be a relatively complicated process. Therefore, the one-to-one binding model is not always valid. (Neubig *et al.* 2003)

Overall, there are two main categories of methods: one that uses radiolabels and the other that uses fluorescent labels. Although there are possibilities that ligand binding can be investigated based on the structure of the receptor protein, but these have not been widely used.

1.2.1. Radioligand binding assay

One of the most widely used methods in GPCR research has been the radioligand binding assay first used by Paton and Rang (Paton and Rang 1965). The radioligand binding assay has been used for a long time and has become a standard in the GPCR field due to its reliability and simple assay format. The measured signal comes from the energy released from the radioactive decay process, which can be detected more sensitively than a chemical process. Therefore, the radioactive isotope can be present in low concentrations, and sensitive radiation detectors and scintillation counters can still detect its presence. However, radioactive decay is a random event and follows an exponential decay. Hence, it releases energy even when it is not being measured, making it potentially harmful to the environment and human health.

The assay is conducted so that the radioligand is first incubated with the receptor, and afterwards, the free ligand is separated from the receptor-bound ligand by centrifugation or filtration. The radioactivity of the bound ligand is measured, and from that, the binding parameters- like K_d, K_i or B_{max} can be calculated. The kinetic parameters cannot be easily obtained because the classical assay is designed in an equilibrium end-point format. Scintillation proximity assay can be used to overcome this problem (Hart and Greenwald 1979). This

alternative method needs the receptor to be immobilised to the surface of scintillation beads. In this homogeneous assay, only the radioligand, which is bound to the receptor and is close to the bead, can excite the scintillation beads and produce photons detectable by the scintillation counter. (Flanagan 2016)

Various radioisotopes are available for labelling ligands with minimal chemical structure modifications and therefore do not affect the receptor-ligand binding affinity. Furthermore, many high-affinity ligands are commercially available, allowing a relatively quick assay set-up. The main isotopes used are ^{3}H, ^{32}P, ^{35}S or ^{125}I, which have varying half-lives and different types of radioactive decay. As hydrogen is always present in organic molecules, labelling ligands by switching a hydrogen atom for a tritium atom is usually easy. However, it is low energy and has long half-lives, resulting in relatively low detection efficiency. On the other hand, ^{125}I has a short half-live (60 days), but it is not a typical atom, and the experiments need to be conducted in a brief timeframe (~6 weeks). Furthermore, as the energy released is larger, it is also more harmful to people. (Flanagan 2016)

The receptor source is the other crucial feature to consider for the radioligand binding assay. Receptor density or concentration must be high enough to give a measurable, specific binding signal that should be higher than the non-specific binding signal. On the other hand, too high amount of the receptor depletes the radioligand, complicating ligand affinity calculation. At first, radioligand binding assays were performed with tissues or tissue preparations, following cell culture preparation and whole cells. Using whole cells preserves the cellular membrane architecture and may save preparation time for chemically or structurally unstable receptors. Binding assays can also be performed using cells attached to culture wells or tissue slices attached to slides (Flanagan 2016). One of the newest possibilities is purified and reconstituted receptors. Usually, a recombinant receptor is expressed in a cell line and then purified for further experiments. The difficulty of this approach is the extraction of the receptors from their native environment in the plasma membrane, as GPCRs are inherently unstable in the detergents required for their solubilization (Jamshad *et al.* 2015). After the complicated purification process, it is necessary to reconstitute the receptors into a lipid structure, mimicking the plasma membrane.

As the GPCR concentration in tissues and primary cells is relatively low and multiple different GPCRs are usually expressed in each tissue, sufficient sensitivity and specificity are difficult to achieve. Thus specific receptors can be expressed in cells with transfection. *Spodoptera frugiperda* (Sf9) insect cells are a convenient option for this application because of their efficient expression. The drawback of a deficient signal transduction system but G-proteins can also be added with transfection (Tõntson *et al.* 2014). However, it should be taken into account that insect and mammalian cells' plasma membrane lipid composition is different. The main steroidal component of the mammalian cell membrane is cholesterol, while insect cells contain ergosterol. (Makela and Oker-Blom 2008).

For a long time, Sf9 insect cell membranes have been used as a good, simple, and relatively inexpensive preparation for obtaining receptors. Since viruses are

already used for transfection and receptor production, viruses multiply and finally bud out from the cells covered with cell membranes containing receptors (Loisel *et al.* 1997). Budded baculoviruses (BBV) particles are produced with Sf9 insect cells using *Autographa californica* multiple nucleopolyhedrovirus. BBVs are rod-shaped particles 200-400 nm in length and 40–50 nm in diameter. They can be easily separated from Sf9 cells by centrifugation and employed as a source of receptors for ligand binding assays, like radioligand assay (Allikalt and Rinken 2017) and FA (Veiksina *et al.* 2014). Baculoviruses (BV) infect many insect species but do not propagate in any vertebrate hosts like humans, so only Biosafety level 1 is needed. Due to the low biohazard risk and ease of use, the baculovirus-insect cell expression system has become widespread (Kost *et al.* 2010). Virus particles start to bud from the Sf9 cell during the BV infection cycle. The virus particles become enveloped by the host's plasma membrane during budding. Therefore, the baculovirus-insect cell expression system represents a versatile tool for displaying recombinant GPCRs on the surface of Sf9 cells and BBV particles. Furthermore, the GPCRs on the surface of BBV particles have their native conformation, orientation and environment.

1.2.2. Fluorescence anisotropy assay

Many optical methods have emerged as alternatives to radioactivity-based assays. The simpler ones are colourimetric, but these are not as sensitive as fluorescence or chemo- and bioluminescence-based assays. Many different readouts can be obtained from fluorescence-based assay to investigate ligand binding to GPCRs, for example, fluorescence intensity (FI), fluorescence anisotropy (FA), fluorescence correlation spectroscopy (FCS) and (Förster/bioluminescence) resonance energy transfer (FRET/BRET). (de Jong *et al.* 2005)

FA method detects the change in rotational diffusion of the fluorescent ligand when it binds to the receptor. It is based on the phenomenon that upon excitation with polarised light, fluorophores whose dipole is parallel to the plane of polarised light will first absorb this light and emit it after a delay depending on the fluorescence lifetime. The emitted light will be partially polarised, whereas polarisation depends on the fluorophore's freedom of rotational diffusion during its fluorescence lifetime (Lakowicz 2006). FA is increased when a low molecular weight fluorescent ligand with high rotational freedom binds to the larger receptor with low rotational freedom. The Perrin equation describes FA as follows:

$$r\,(\tau) = \frac{r_0}{1+\frac{\tau}{\tau_c}} \qquad (1)$$

where r is the observed anisotropy, r_0 is the intrinsic anisotropy of the molecule, τ is the fluorescence lifetime, and τ_c is the rotational correlation time (Perrin 1929). (Jablonski, A 1960; Rinken *et al.* 2018)

As FA does not require separation of the free ligand from receptor-bound ligand for measurement, this enables easy kinetic measurements. Therefore, K_d

can be obtained from both kinetic and equilibrium end-point experiments. Kinetic data gives more information about the ligand-receptor complexes' formation and dissociation. However, it should be noted that FA experiments are not performed with an excess of the probe thus, pseudo-first-order reaction conditions are not met. Therefore, ligand depletion and second-order kinetics have to be considered in most cases. (Rinken *et al.* 2018)

Since fluorescent labels are much more complex than radioisotopes, developing a new fluorescent ligand is more complicated compared to a radioligand. Fluorescent labelling is more difficult because the ligand structure is significantly altered by adding a large label. Furthermore, to maintain the affinity of the starting compound, the derivatization should be done by considering the structure of the receptor-ligand complex. As crystallisation and cryo-EM have been used to solve more and more GPCR structures, it becomes easier to design new fluorescent ligands (Shimada *et al.* 2020). After understanding where the linked and the dye should be positioned, a suitable dye should be chosen, as many options have become available. One of the first parameters to consider is excitation and emission wavelengths. The red-shifted dyes like Cy3B and 5-TAMRA are preferred, as the autofluorescence is generally lower in this part of the spectrum. The other important parameter to be considered for FA assay is fluorophore's fluorescence lifetime – for low molecular weight ligands, it should remain between 2 – 5 ns. Furthermore, a fluorescent label should also have a high extinction coefficient, quantum yield, stability, and low bleaching and non-specific binding. (Rinken *et al.* 2018)

At first, membrane preparations were used, and a sound signal output could be achieved (Veiksina *et al.* 2010). However, lipoparticles in the membrane preparations have a variable size and uncontrolled receptors' orientation. Therefore, alternative receptor sources have been used, such as solubilised receptors, reconstituted into lipid vesicles. These approaches solve the issue of particle size but are relatively time-consuming, thus unsuitable for HTS applications. The BV system is an easy way to produce a large number of particles with a uniform size. Therefore, BBVs are more suitable for FA assay. Furthermore, the small size of BBV particles prevents their fast sedimentation. Thus, a stable signal can be obtained for at least 12h (Veiksina *et al.* 2014; Link *et al.* 2017;). (Rinken *et al.* 2018)

1.2.3. Förster resonance energy transfer sensors

FRET is a non-radiative energy transfer between two chromophores, an energy donor and an energy acceptor. For FRET to occur, three conditions have to be met: 1) the distance between the donor and the acceptor should be small ($\leq$ 10 nm); 2) the donor emission spectrum and the acceptor absorption spectra must overlap; 3) the correct orientations of the donor emission dipole moment and the acceptor absorption dipole moment. (King *et al.* 2012)

FRET-based biosensors have been developed for essentially all steps in GPCR-mediated signalling. These sensors are based on either conformational

changes within proteins, such as the agonist-dependent activation of receptors and cAMP recognition or molecule-molecule interactions, such as the G-protein coupling to the receptor or ligand binding to the receptor. For the sensors to work, both the donor and the acceptor must be inserted at suitable sites in the relevant proteins. However, most of these assays are not suited for HTS, as the signal is small because of the high background autofluorescence. (Lohse *et al.* 2012)

1.2.4. Bioluminescence resonance energy transfer assay

Unlike in FRET, autofluorescence is not a factor in BRET. BRET method is based on the RET occurring in some marine species, for example, in the sea pansy, *Renilla reniformis*. This method was initially developed to study the interactions of circadian clock proteins in bacteria, but the application range has widened drastically. In BRET, the luciferase enzyme catalyses a specific reaction in which a substrate is converted into a product in an excited state. Such a product acts as an energy donor. When used for the ligand-binding assay, the energy acceptor is a fluorescent ligand, absorbing energy released from the reaction and reemitting light at a longer wavelength. (Bacart *et al.* 2008)

The first step for developing a BRET-based ligand-binding assay is labelling the receptor of interest with a luciferase. This is usually done at the N terminus to ensure that the luciferase remains on the extracellular side because the fluorescent ligand binds to the extracellular regions of the receptor. Various luciferase variants have been utilised as donors, such as firefly luciferase (FLuc), derived from the North American firefly *Photinus pyralis* and Renilla luciferase (RLuc), derived from the sea pansy *Renilla reniformis*. However, their high molecular weight (61 and 38 kDa) makes them unfit for labelling the N-terminal of a receptor. Alternatively, smaller 19 kDa luciferase NanoLuc was engineered from deep-sea shrimp *Oplophorus gracilirostris*. NanoLuc is more stable and produces a significantly brighter and sustained luminescent signal than the previous variants. Furthermore, the original substrate utilised by *Oplophorus gracilirostris* was also improved to get a 30-fold brighter signal. (Stoddart *et al.* 2018)

1.2.5. Flow cytometry

Flow cytometry was developed in the 1960s to analyse and sort cell populations. Flow cytometry can measure a single cell's or other particle's optical and fluorescence characteristics in a fluid stream when it passes through a light beam. However, a flow cytometer can assess thousands of particles per second. Therefore, population statistics can be still measured in a reasonable time. Flow cytometry enables the cell population analysis and purification based on fluorescent or light scattering characteristics. The parameters obtained from the experiment are based on the optical set-up. Light scattering is directly related to the size and morphological properties of the cell. However, fluorescence emission caused by a fluorescence probe is proportional to the amount of fluorescent probe

bound to the cell. This makes flow cytometry a diverse method that can also be used to characterise new ligands. (Waller *et al.* 2004; Adan *et al.* 2017)

1.2.6. Microscopy assays

Fluorescence microscopy equipment has become more affordable and, therefore, more common. Also, the growing number of fluorescent labels and labelling techniques have made it easy to use. Thus, fluorescence microscopy has been frequently used in scientific studies, but mainly qualitatively. Compared to most spectroscopy methods, microscopy images contain a large amount of data, complicating the quantitative data analysis. Hence, it has rarely been used in ligand binding assays.

One of the few studies for this kind of microscopy application is used to study muscarinic acetylcholine receptor subtype M_1 using an IsoCyte™ laser scanning platform (Lee *et al.* 2008). The experiments were conducted with live cells with Cy3B-telenzepine in a simple no-wash protocol using the novel optics and confined detection region of the IsoCyte™ laser scanning platform in an HTS-compatible format. However, the image analysis was done in a relatively straightforward manner. First, from the pixel intensity histogram analysis, the background for each image was determined. Considering the background fluorescence, the threshold was set to a constant value above the background level. Then to calculate the fluorescence intensity, the grey-scale values of all pixels above the threshold were summed and the background corrected. The flaw of this kind of analysis is the underrepresentation of low-intensity cells. Furthermore, there is no normalization for the number of cells. Therefore, the number of cells in the image significantly influences the results.

To improve the microscopy-based assay, a more detailed analysis is needed. This can be done by manually drawing the region of interest around the plasma membrane or using another fluorescence marker to identify all cells (Stoddart *et al.* 2012). Manual cell detection takes much time or loss in the number of cells used for analysis. Using a modified receptor to find all the cells is more accessible because fluorescence images can be used, but adding a modification, like a YFP, may influence ligand binding and receptor activation. Also, total intensity methods must consistently seed cells as a high confluency monolayer, but this is either difficult or practically impossible with some cell lines, like the HEK-D3R cells (Allikalt *et al.* 2021). Moreover, dense monolayers can significantly affect physicochemical environmental parameters such as oxygen concentration, directly affecting muscarinic receptor signalling (Place *et al.* 2017; Mou *et al.* 2006).

Furthermore, these problems were addressed by using brightfield images to find all the cells or even only the cell membranes (Allikalt *et al.* 2021). Overall, brightfield images are more complicated to analyse because there can be more than just the object of interest and finding the object without a maker is also more difficult. Identifying individual cells from a dense monolayer is more challenging, so fewer cells are needed for this analysis. The membrane detection

algorithm developed as a part of the live-cell assay was only used for HEK-D3R cells and in saturation and competition binding assays, so there is a need for further improvements.

All things considered, moving to more natural systems for HTS ligand binding assays will give a more comprehensive understanding of ligand-receptor interactions. Nevertheless, this development should not come with a sacrifice of kinetic parameters or measurement speed.

2. AIMS OF THE STUDY

The general aim of the study is to find new possibilities to study ligand binding properties for different GPCRs. This included:

- Implementation of FA assay for studies of different GPCRs
- Development of TIRF-based assay for study fluorescent ligand binding to GPCRs in budded baculoviruses
- Development of live-cell microscopy assay for characterisation of fluorescent ligand binding to GPCRs
- Characterisation of the effects of different modulators on GPCRs by different fluorescence-based assays.

3. MATERIALS AND METHODS

3.1. Cell lines and reagents

Spodoptera Frugiperda (Sf9) cells (Invitrogen Life Technologies) were grown as a suspension culture in antibiotic- and serum-free growth medium EXCELL® 420 (Sigma-Aldrich) at 27 ºC in a non-humidified incubator.

Chinese hamster ovary (CHO-K1) cells (ATCC®, LGC Standards) were modified to stably express human wild-type melanocortin MC_4 receptors (**PAPER III**). Both naive and modified CHO-K1 cells were grown as an adherent monolayer culture in high glucose Dulbecco's Modified Eagle's Medium (DMEM) (Sigma-Aldrich) supplemented with 10% fetal bovine serum (FBS) (Sigma-Aldrich), 100 U/mL penicillin, 0.1 mg/mL streptomycin (PAA Laboratories). For cells with MC_4 receptors also, 400 µg/ml of geneticin was added. CHO-K1 cells expressing muscarinic acetylcholine M_4 receptor were purchased from Missouri S&T cDNA Resource Centre. They were cultured in HAM's F12 medium supplemented with FBS (9%), antibiotic antimycotic solution (100 U/mL penicillin, 0.1 mg/mL streptomycin, 0.25 µg/mL amphotericin B) (Sigma-Aldrich) and geneticin (750 µg/mL). MCF-7-Y1 cells were established by (Keller *et al.* 2011) and cultivated in EMEM containing 5% FBS and antibiotic antimycotic solution. To increase the Y1 receptor expression, the MCF-7-Y1 cells were incubated with 1 nM 17b-estradiol 48-72 h before the experiment. All mammalian cells were grown at 37 ºC in a humidified incubator with 5% CO_2 until 80-100% confluency and then reseeded.

Cell culture viability and density were determined with an Automated Cell Counter TC20™ (Bio-Rad Laboratories) by adding 0.2% trypan blue (Sigma-Aldrich).

Assay buffer (AB) consisted of MilliQ water, 135 mM NaCl (AppliChem), 1 mM $CaCl_2$ (AppliChem), 5 mM KCl (AppliChem), 1 mM $MgCl_2$ (AppliChem), 11 mM Na-HEPES (pH = 7.4) (Sigma-Aldrich), protease inhibitor cocktail (according to the manufacturer's description, Roche) and 0.1% Pluronic® F-127 (Sigma-Aldrich). Metal ion effects were studied using ethylenediaminetetraacetic acid (EDTA, Merck), $ZnSO_4$ (ReaChim), and $CuCl_2$ (Sigma-Aldrich). For experiments with neuropeptide Y (NPY) Y_1 receptors, KCl and $MgCl_2$ were not added to AB.

All ligand stock solutions were prepared using dimethyl sulfoxide (DMSO) (AppliChem) cell culture grade and stored at -20 °C. Unlabelled ligands of MC_4 receptors were purchased from Tocris Bioscience (NDP-α-MSH, SHU9119, HS024). Muscarinic acetylcholine receptor ligands acetylcholine, arecoline, pirenzepine, pilocarpine, atropine, and scopolamine were purchased from Sigma-Aldrich, carbachol from Tocris Bioscience (Abingdon, United Kingdom). NPY receptor ligands BIBO 3304 (R&D Systems), PYY (BioNordika), and pNPY (Synpeptide) were purchased. All the following ligands were all synthesised at the University of Regensburg and kindly provided by Dr Max Keller:

- UR-MK342 compound 20 in (Gruber *et al.* 2020) – 2-(6-(Dimethylamino)-3-(dimethyliminio)-3H-xanthen-9-yl)-5-((2-(4-(4-(1-(2-oxo-2-(11-oxo-10,11-dihydro-5H dibenzo[b,e][1,4]diazepin-5-yl)ethyl)piperidin-4-yl)butyl)piperazin-1-yl)ethyl)carbamoyl)benzoate tris(hydrotrifluoroacetate)
- UR-CG072 compound 15 in (Gruber *et al.* 2020) – 2-(6-(Dimethylamino)-3-(dimethyliminio)-3H-xanthen-9-yl)-5-((2-(3-(1-(4-(1-(2-oxo-2-(11-oxo-10,11-dihydro-5H-dibenzo[b,e][1,4]diazepin-5-yl)ethyl)piperidin-4-yl)butyl)-1H-imidazol-4-yl)propanamido)ethyl)carbamoyl)benzoate bis(hydrotrifluoroacetate)
- UR-SK59 compound 64 in (She *et al.* 2017) – N1-(2-(4-(2-Oxo-2,3-dihydro-1H-benzo[d]imidazol-1-yl)-[1,4'-bipiperidin]-1'-yl)ethyl)-N3-(2-(4-(4-(1-(2-oxo-2-(11-oxo-10,11-dihydro-5H dibenzo[b,e][1,4]diazepin-5-yl)ethyl)piperidin-4-yl)butyl)piperazin-1-yl)ethyl)-5-(propionamidomethyl)isophthalamide pentakis(hydrotrifluoroacetate)
- UR-SK75 compound 46 in (She *et al.* 2017) – 5-(2-(4-(4-(4-(3-((4-(1-Methyl-1,2,5,6-tetrahydropyridin-3-yl)-1,2,5-thiadiazol-3-yl)oxy)propyl)piperazin-1-yl)butyl)piperidin-1-yl)acetyl)-5,10-dihydro-11H-dibenzo[b,e][1,4]diazepin-11-one tetrakis(hydrotrifluoroacetate)
- UNSW-MK259 compound 62 in (Keller *et al.* 2015a) – 5-((4-(4-(4-(((N-(2-Propionamidoethyl))-3-amino-3-oxo)propyl)1H-imidazol-1-yl)butyl)piperidin-1-yl)acetyl)-5H-dibenzo[b,e][1,4] diazepin-11(10H)-one
- UR-MC026 compound 40 in **PAPER IV** – 5-{[4-(4-{(1R,4R,Z)-9-Amino-4-[(4-hydroxybenzyl)carbamoyl]2,11,16-trioxo-1-phenyl-3,8,10,12,15-pentaazaoctadec-9-en-1-yl}phenoxy)butyl]carbamoyl}-2-[6-(dimethylamino)-3-(dimethyliminio)-3H-xanthen-9-yl]benzoate Hydrotrifluoroacetate
- CM159 compound 39 in **PAPER IV** – 5-{[4-(3-{(1S,4R,Z)-9-Amino-4-[(4-hydroxybenzyl)carbamoyl]2,11,16-trioxo-1-phenyl-3,8,10,12,15-pentaazaoctadec-9-en-1-yl}phenoxy)butyl]carbamoyl}-2-[6-(dimethylamino)-3-(dimethyliminio)-3H-xanthen-9-yl]benzoate Hydrotrifluoroacetate
- CM139 compound 37 in **PAPER IV** – 4-(2-{(1E,3E)-5-[(Z)-1-(6-{[4-(3-{(1S,4R,Z)-9-Amino-4-[(4hydroxybenzyl)carbamoyl]-2,11,16-trioxo-1-phenyl-3,8,10,12,15pentaazaoctadec-9-en-1-yl}phenoxy)butyl]amino}-6-oxohexyl)3,3-dimethyl-5-sulfoindolin-2-ylidene]penta-1,3-dien-1-yl}-3,3-dimethyl-3H-indol-1-ium-1-yl)butane-1-sulfonate Hydrotrifluoroacetate
- CM138 compound 35 in **PAPER IV** – 4-{(1E,3E)-4-[4-(Dimethyl-amino)phenyl]buta-1,3-dien-1-yl}-1-[4(3-{(1S,4R)-4-[(4-hydroxybenzyl)carbamoyl]-9-imino-2,11,16-trioxo-1-phenyl-3,8,10,12,15-pentaazaoctadecyl}phenoxy)butyl]-2,6dimethylpyridin-1-ium Hydrotri-fluoroacetate Trifluoroacetate
- UR-MK299 compound 38 in (Keller *et al.* 2015b) – (R)-Nα-Diphenylacetyl-Nω-[2-([2,3-3H]propionylamino)ethyl]aminocarbonyl-(4-hydroxybenzyl)argininamide

3.2. Budded baculovirus preparation

A detailed guide for making BBV is given in **PAPER I,** and all BBV were produced similarly with minor modifications in restriction sites, transfection reagents and MOI used in amplification. The MC_4, M_2, M_4, and Y_1 receptor genes in pcDNA3.1+ were purchased from the cDNA Resource Center (www.cdna.org). Then the cDNA of the GPCR of interest was subcloned into the appropriate restriction site of the pFastBac1 vector under the control of the polyhedrin promoter and transformed into DH10Bac-competent cells. Next, recombinant bacmid DNA was purified with a commercial kit and used to generate recombinant baculovirus via transfection of Sf9 cells with commercial transfection reagents. After the viruses were generated and collected, the amount of infectious viral particles per mL (ivp/mL) for all the baculoviruses was determined with the Image-based Cell Size Estimation (ICSE) assay (Laasfeld *et al.* 2017). The viruses were amplified to get a high ivp/mL virus used to make BBV particles for FA and TIRF experiments. To produce the BBV particles, Sf9 cells were infected with MOI = 3-5 and incubated for 3-5 days (end viability of Sf9 cells was below 55%). The supernatant containing BBV particles was gathered by centrifugation for 15 min at 1600 g. Next, the BBV particles were concentrated 40-50-fold by high-speed centrifugation (48000 g at 4 °C) for 40 min, followed by washing with the AB and homogenisation with a syringe and a 30G needle. The suspension was divided into aliquots and stored at -90 °C until the experiments.

3.3. Fluorescence anisotropy assay

A detailed description of the FA assay is given in **PAPER I**. The FA experiments were performed on black flat bottom half-area 96 well plates (Corning, Glendale, USA) with a final volume of 100 µL/well or 110 µL/well in the case of NPY Y1 TIRF assay (**PAPER V**).

Briefly, in saturation binding experiments, two concentrations of fluorescent ligands were used with a 2-fold dilution of BBV particles and a non-labelled competitive ligand with a 1000-times higher concentration was used to determine non-specific binding. For competition binding experiments, the concentrations of fluorescent ligand and the volume of BBV particles was also kept constant. All the specifics can be found in the respective papers.

FA measurements were performed with a multi-mode plate reader Synergy NEO (BioTek Instruments, Winooski, USA), which is equipped with a polarising 530(25) nm excitation filter and 590(35) nm emission filter allowing simultaneous parallelly and perpendicularly polarised fluorescence detection.

3.4. cAMP assay

For measuring the biological response of ligand binding to MC_4 receptors, a fourth-generation genetically encoded FRET-based biosensor $Epac^{H187}$ was used. Dr Kees Jalink kindly provided this sensor, and the cloning into the BacMam system is described in **PAPER II**.

For measuring the cAMP, change was measured in CHO-K1-MC4R cells. To express the $Epac^{H187}$ biosensor cells were treated with the BacMam viral stock (MOI: 9–25) in a growth medium containing 12 mM sodium butyrate (Sigma-Aldrich) and seeded on a black clear-bottom 96-well cell culture plate (Corning Life Sciences) at the density of 1×10^5 cells/well in a 100 µL volume. The cells were incubated for 30 h at 30°C in a humidified CO_2 incubator (5%) for recombinant protein production. The growth medium with BacMam virus and sodium butyrate was replaced with an AB without $CaCl_2$. The palate was measured once before the ligands or ions were added to obtain the baseline. The assays were performed on a Synergy™ NEO microplate reader (BioTek), with excitation at 420/50 nm and simultaneous dual emission at 485/20 nm and 540/25 nm. The change in FRET values was calculated as follows (Mazina *et al.* 2012) :

$$\Delta\mathrm{FRET} = \frac{\frac{I^A_{t=0}}{I^D_{t=0}} - \frac{I^A}{I^D}}{\frac{I^A_{t=0}}{I^D_{t=0}}} \qquad (2)$$

The $I^A_{t=0}$, $I^D_{t=0}$, and I^A, I^D refer to the fluorescence emission intensities of the acceptor and donor fluorophores before and after cell stimulation, respectively.

3.5. TIRF microscopy and assay set up with BBVs

The TRIF microscope is custom made with details described in **PAPER IV** and **V**. Briefly, the imaging was done with Olympus 60× APON NA 1.49TIRF objective and ET 605/70 m emitter filter (Chroma) by Dr Sergei Kopantšuk.

Also, the same microscope was used by Dr Sergei Kopantšuk for measurements of MCF-7-Y1 cells in **PAPER IV**. MCF-7-Y1 cells were seeded at a density of 20000 cells per well into eight-well CG imaging chambers (Zell Kontakt GmbH, Germany). After incubation for 24 h in EMEM (Sigma) supplemented with 1 nM estradiol, FCS (Sigma), and a solution containing penicillin (100 units/mL), streptomycin (0.1 mg/mL), amphotericin B (0.25 µg/ mL) (Sigma), and nuclear stains [5 µg/mL Hoechst 34580 (Chemodex Ltd., St. Gallen, Switzerland) or 1 µM SiR-DNA (Spirochrome AG, Stein am Rhein, Switzerland)] was added, and incubation was continued for 1 h. The culture medium was replaced with LiveLight MEMO imaging medium (Cell Guidance Systems, Cambridge, U.K.) (200 µL, supplemented with supplement A according to the manufacturer's protocol). After incubation for 2 h at 37 °C in a humidified

atmosphere containing 5% CO_2, compounds fluorescent ligands CM159, CM138, CM139 with 1 nM final concentrations were added, and cells were imaged for ≤60 min (37 °C, atmosphere with 5% CO_2).

All samples for the TIRF assay with NPY Y_1 BBV were prepared in the 96 well half-area, flat-bottom polystyrene NBS microtiter plates as previously described in the FA assay part with a final volume of 110 µL because 50 nM neutravidin and cholesterol-PEG-biotin were also added (**PAPER V**). After measuring FA for 20 µL of the solution from the 96 well plate was transferred to the corresponding wells of the 48 multiwell-system developed by Robin Benjamin Ehrminger. Coverslips with the dimensions 22 mm × 22 mm × 170 ± 5 µm (thickness no. 1.5H) were bought from Marienfeld Precision (LaudaKönigshofen, Germany) and treated and attached as described in **PAPER V** by Tõnis Laasfeld.

3.6. Live-cell fluorescence microscopy assay

CHO-K1-hM_4R cells were seeded into µ-Plate 96 well Black plate (Ibidi) at densities of 25 000 – 55 000 cells/well in DMEM/F-12 medium and incubated for 5-7 h. Immediately before the measurement, the cell culture media was exchanged for the same cell culture media containing ligands. At all times, the well liquid volume was kept at 200 µL.

For determining UR-CG072 affinity to the M_4 receptor, saturation binding experiments were carried out using two-fold dilutions of UR-CG072 starting from 8 nM. Non-specific binding was measured in the presence of 3.7 µM scopolamine. The cells were incubated with ligands in Cytation 5 at 5% CO_2 and 37 °C for 2 h before imaging.

For measuring UR-CG072 binding kinetics to the M_4 receptor, 2 nM UR-CG072 was added to the cells, and imaging was immediately initiated. To achieve sufficient temporal resolution, only two wells were imaged in parallel. After approximately 3 h of association, 10 µL of 100 µM scopolamine (C_{final} = 5 µM) was added to start dissociation.

The competition binding assay was performed using 2 nM UR-CG072. It was determined that 2 h was sufficient to reach equilibrium for IC_{50} value measurement as the IC_{50} values for scopolamine and carbachol at 2 h and 5 h remained constant within uncertainty limits.

The cells were imaged with Cytation 5 cell imaging multi-mode plate reader equipped with 20X LUCPLFLN objective (Olympus) from Bright-field and RFP channels (LED light source with excitation filter 531(40) nm and emission filter 593(40) nm for RFP channel (BioTek Instruments). Specifications of parameters are in **PAPER VII**. The cells were imaged in the montage mode (4 locations/ well) with Z-stack (10 planes, 4 planes below focal plane, 1 in focus and 5 planes above focal plane).

3.7. Data analysis

Aparecium 2.0 software was developed in our laboratory by Tõnis Laasfeld and is available at www.gpcr.ut.ee/software.html. It was used to blank the raw parallel and perpendicular intensity values and calculate the FA values using the formula:

$$FA(t) = \frac{I(t)_{II} - I(t)_{\perp}}{I(t)_{II} + 2 \cdot I(t)_{\perp}} \quad (3)$$

where $I(t)_{II}$ is the parallel fluorescence intensity, and $I(t)_{\perp}$ is the perpendicular fluorescence intensity at time point t.

The TIRF microscopy images were analysed with Apareciums SPOT Normalized Intensity Calculator (SPOTNIC) toolbox. For cell detection from brightfield images, Aparecium toolbox MembraneTools was used.

Graphpad Prism 5.04 (GraphPad Software, San Diego, USA) was applied to fit and obtain the $logIC_{50}$ values with a built-in model "log(agonist) vs response". To obtain k_{on} and k_{off} form kinetic data "Association then dissociation" model was used. K_d calculation from microscopy saturation data was done with the model "One site – Total and non-specific binding". To calculate K_d from FA data, a global model form (Veiksina et al. 2014) was used to take ligand depletion into account

For LoD and LoQ determination, the highest concentration among all experiments of either Y_1 receptor or UR-MC026 concentration variation surpassed the 3 SD and 10 SD difference between respective total, and non-specific measurement points were set as the LoD and LoQ values, respectively.

All the data are presented as the mean ± standard error of the mean of at least three independent experiments if not stated otherwise. However, all the results from **PAPER VII** are weighted averages, and all the uncertainties given are weighted standard error of the mean of at least 3 independent experiments if not stated otherwise.

4. RESULTS AND DISCUSSION

4.1. Fluorescence anisotropy assay development

The general aim of the thesis was to find new possibilities to study ligand binding properties for different GPCRs. During the last decade, we have worked on the implementation of FA assays to study fluorescence ligand binding to dopamine (Allikalt *et al.* 2018), melanocortin (Veiksina *et al.* 2014; Link *et al.* 2017) and serotonin 1A (Tõntson *et al.* 2014) receptors. In this thesis, the application range has been extended with the addition of NPY Y_1 (**PAPERS IV** and **V**) and two muscarinic acetylcholine receptor subtypes: M_2 (**PAPER VI**) and M_4 (**PAPER VII**).

Our workgroup first used BBVs as the receptor source for FA assay in 2014 (Veiksina *et al.* 2014), and a year later first detailed protocol of this method was published (Veiksina *et al.* 2015). Later in 2018, a detailed theory behind FA assay and what kind of information cloud be obtained was described (Rinken *et al.* 2018). However, as time passed and new knowledge was gained, an updated version of the protocol was needed. Therefore, an up-to-date protocol with a step-by-step guide for setting up and conducting FA assay with BBV as the receptor source was published (**PAPER I**). Including a guide for data analysis and tips on how to get the most information from this data. This publication is an excellent tool for disseminate the knowledge our lab has gained over more than 10 years of developmental work on FA assay.

Figure 1 gives an overview of how this assay is conducted. The assay set-up starts with making BBVs, which requires multiple cloning steps. The cloning starts with cutting the cDNA of the receptor of interest out of the vector with suitable restriction enzymes and then inserting it into the pFastBac vector under the polyhedrin promoter. Next, this construct is inserted into a shuttle vector (bacmid) with site-specific transposition. Using a commercial transfection reagent the bacmid is inserted into Sf9 cells. Now, the cells start producing the receptor of interest and new baculoviruses. The baculoviruses are released by budding out of the cell, thus taking part of the membrane with them. BBVs are concentrated, washed and stored at -90 °C for the experiments.

FA-based ligand binding assays were carried out on microplates where BBV and fluorescence ligand are mixed. FA of the fluorescence ligand-receptor complex is higher than the free ligand FA. As fluorimeter can measure FA values of all wells of the plate, we get information about ligand binding level, and its kinetics for all samples studied. Data management was performed with the software Aparecium, developed in our laboratory for multiple assay types and is compatible with several fluorescence plate readers. Aparecium has a graphical user interface that enables easy data transformations and exports it to other programs like GraphPad Prism or SBToolbox2.

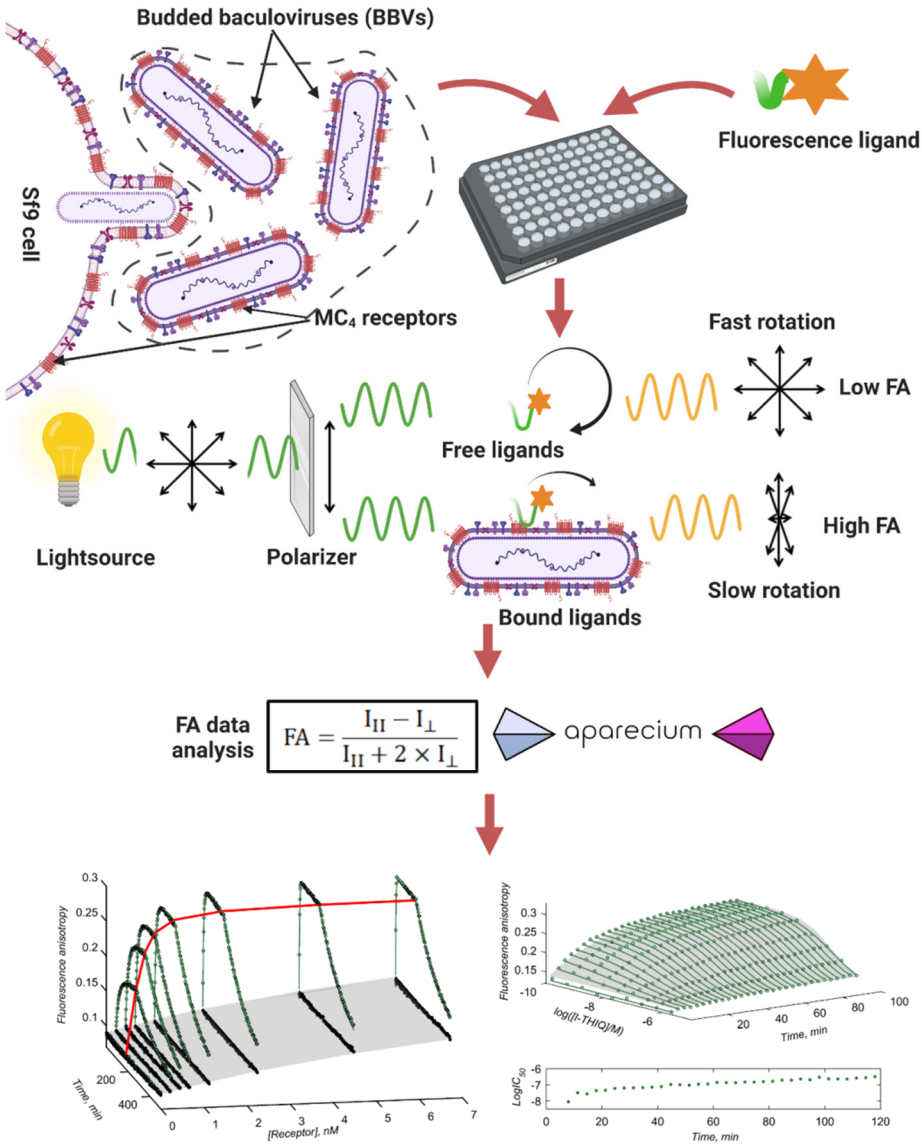

Figure 1 General set-up of fluorescence anisotropy (FA) based ligand binding assay, using budded baculoviruses as a receptor source. BBVs were obtained from Sf9 (*Spodoptera frugiperda*) cells and carry the recombinant receptors expressed by the host cell. FA-based ligand binding assays were carried out on microplates where BBV and fluorescence ligand were added. Fluorescence ligand binding to the receptors can be characterised by the change in FA values, which were calculated from the experimentally measured fluorescence intensities that are parallel (I_I) and perpendicular ($I_\perp$) to the polarization plane of excitation light. FA values are low when fluorescence ligands molecules are free in the solution and high when fluorescent ligands are bound to the receptor. Data analysis was conducted with Aparecium.

4.2. cAMP assay development

The signal transduction is an essential part of normal GPCR functioning. One of the most well-known pathways is the cAMP pathway, in which cAMP concentration is increased by G_s activation and decreased by G_i activation. There are many ways to measure this change, and we are using genetically encoded FRET-based biosensors developed by Dr Kees Jalink from the Netherlands Cancer Institute. However, the first generation of these kinds of sensors was developed based on exchange protein directly activated by cAMP (Epac) and cAMP-dependent protein kinase (PKA) in Dr Martin Lohse's workgroup (Nikolaev *et al.* 2004). In our workgroup, this Epac2-camps biosensor was also successfully applied for studies of Melanocortin MC_1 receptor activation (Mazina *et al.* 2012). In the next generation of biosensors, the fluorescent proteins were switched out, but the cAMP binding domain stayed the same (Klarenbeek *et al.* 2011). This new sensor Epac-S^{H74} was used in our lab to generate a detailed protocol to standardise the cAMP assay (Mazina *et al.* 2015). However, fourth-generation Epac-S^{H188} and Epac-S^{H187} biosensors with somewhat higher affinity were developed (Klarenbeek *et al.* 2015). Therefore an updated protocol was also needed.

In **PAPER II** a standardised protocol was put together for using fourth-generation genetically encoded FRET-based biosensors in live cells to obtain comparable results. It starts with inserting the biosensor DNA into cells. We have chosen BacMam technology over the more common transfection reagents because this yielded more consistent expression levels between independent experiments. However, implementing a new sensor requires several cloning steps to insert the biosensor DNA into a baculovirus DNA. After that step, the baculoviruses are generated in Sf9 cells and the optimisation of the assay with live mammalian cells. All the details are given in an easy-to-follow step-by-step guide in **PAPER II**. Figure 2 summarises the experiment set-up with CHO-MC4R cells after the generation of baculoviruses. The most common parameters to optimise are the amount of virus, the incubation time and temperature. For example, CHO-K1 expressing MC_4 receptors need over 30 h incubation at 30 °C for optimal biosensor expression rather than the usual 24 h at 37 °C.

This assay set-up with the new generation sensor was used to determine the biological response of the human chorionic gonadotropin (hCG) (**PAPER II**). As ligand binding assays for receptors with large endogenous ligands are hard to develop, this biological response assay provides information about the receptor-ligand complex. Furthermore, this assay was used to determine the biological response of novel MC_4 receptor fluorescent ligands UTBC102 and UTBC101 developed in our laboratory and previously used in the FA assay (**PAPERS I and III**). UTBC102 and UTBC101 were partial agonists achieving a 68 ± 5% and 22 ± 2% activation level compared to a full agonist NDP-α-MSH. However, adding the TAMRA label to NDP-α-MSH did not change the biological response's size or the ligand's efficacy. Additionally, in our assay, HS024, which is known to be an antagonist, showed a minimal agonistic effect.

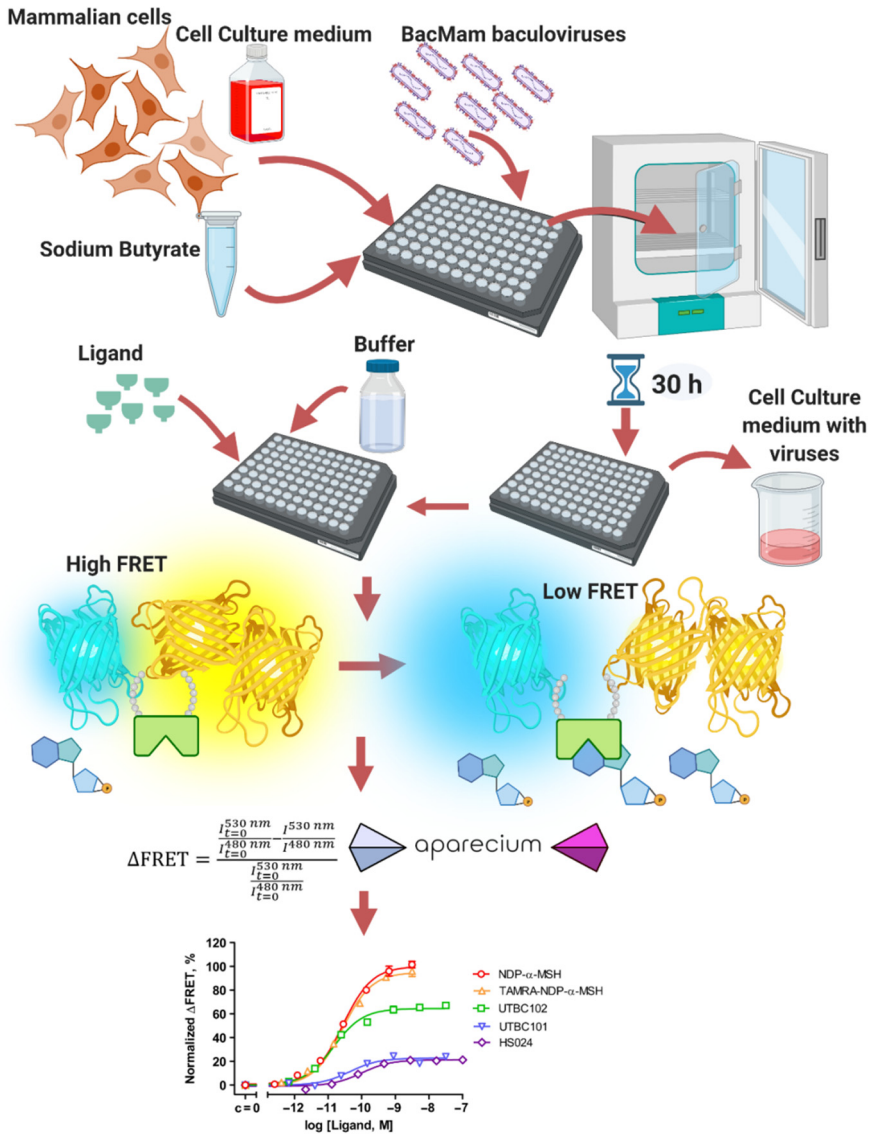

Figure 2 General set-up of cAMP biosensor assay system using BacMam expression system. Cells are seeded to the 96 well plates with BacMam viruses and sodium butyrate and then incubated at 30 °C for 30 h so that the cells can produce the biosensor. Then the cell culture medium is replaced by the buffer, and ligands are added. The genetically encoded consists of mTurquoise donor fluorophore and two cpVenus acceptor fluorophores connected by the Epac domain, which binds cAMP. When the cAMP concentration in cells is low, donor fluorophores can transfer the energy to acceptor fluorophores because they are close together. If the cAMP concentration rises, the Epac domain binds cAMP and donor and acceptor fluorophore to move further apart, and energy transfer does not occur anymore. Using the fluorescent intensity ratio of donor and acceptor

4.3. Modulation of melanocortin 4 receptors by divalent ions

The development of these two standardised assay protocols led to a systematic study in **PAPER III** of MC_4 receptor modulation by metal ions. Ligand binding to MC_4 receptor is known to be a complex system, with known oligomerisation of receptors or a need for Ca^{2+} ions for high-affinity ligand binding. Fluorescence ligand UTBC101 developed in our laboratory (Link *et al.* 2017) was used to study the effect of metal ions on ligand binding. Studying ligand binding in FA assay revealed that Zn^{2+} and Cu^{2+} in the presence of Ca^{2+} inhibit fluorescence ligand binding to the receptor. With a more precise kinetic analysis, it was determined that both Zn^{2+} and Cu^{2+} act as negative allosteric modulators of MC_4 receptors.

Next, the effects of these ions on signal transduction were measured using the biosensor assay for monitoring cAMP concentration change in live cells. From biosensor experiments, it was shown that at low micromolar concentrations, Zn^{2+} caused MC_4 receptor-dependent activation of the cAMP pathway, whereas Cu^{2+} reduced the activity of MC_4 receptors even below the basal level. These findings indicate that at physiologically relevant concentrations, Zn^{2+} and Cu^{2+} can function as MC_4 receptors agonists or inverse agonists, respectively. This complex mechanism could only be discovered by integrating the results of ligand binding and biological response assays based on **PAPER I** and **II** (figure 3).

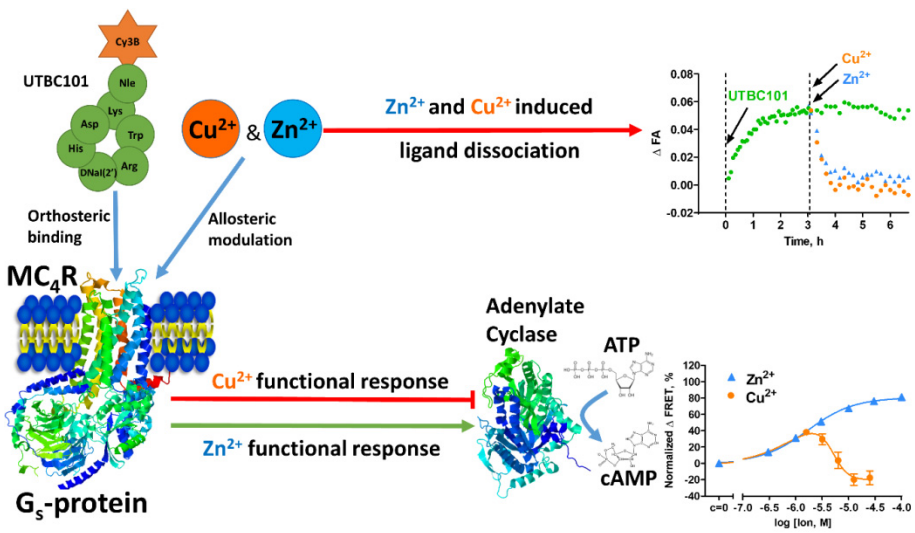

Figure 3 Modulation of Melanocortin 4 receptor by metal ions. Monitoring ligand binding with FA assay showed the dissociation of fluorescent ligand UTBC101 after adding Cu^{2+} and Zn^{2+}. However, monitoring biological response by cAMP concentration change with a FRET-based biosensor showed a different behaviour for Cu^{2+} and Zn^{2+} ions. Zn^{2+} acted as a partial agonist, whereas Cu^{2+} acted as an inverse agonist.

4.4. Characterisation of high-affinity NPY Y_1 receptor ligands

One limitation of FA assays is the small amount of available fluorescent ligands. However, Dr Max Keller and his workgroup have done much work in this field. One of the most critical septs in the development of new ligands is the identification of low molecular weight scaffolds, especially for peptide receptors like NPY receptors. By altering the structure of one of the few known NPY receptor ligands, BIBP3226, they could synthesise several novel high-affinity ligands (Keller *et al.* 2015b; Keller *et al.* 2011; Keller *et al.* 2008) and label one of them with different fluorescent dyes (TAMRA, PY5, CY5) (**PAPER IV**). Different dyes are suitable for different types of biochemical assays. All three ligands showed nanomolar affinities in radioligand binding assay and flow cytometry. In FA assay, mostly red-shifted dyes like TAMRA or Cy3B have been used because of their brightness and suitable fluorescence lifetime. Thus, the TAMRA labelled CM159 was chosen for the characterisation in the FA assay. The obtained K_d value of 9.5 pM was in good agreement with affinity determined with flow cytometry (K_{d_kin} = 4 pM).

Furthermore, CM159 was also used to determine the affinity values for non-labelled NPY Y_1 receptor ligands. Most of the results were in good agreement with the literature, but the K_i could not be accurately determined for endogenous ligand pNPY because the apparent affinity was too low. Also, in flow cytometry assay with CM159 pNPY showed considerably lower affinity than previously reported in the literature. This indicates that these discrepancies cannot be attributed to the used methods but instead to peculiarities of ligand−receptor interactions.

Next, the new fluorescent ligands were used in fluorescence microscopy with live MCF-7 cells expressing the Y_1 receptor. As microscopy does not have the same limitations on fluorophores, ligands with other labels were also tested. However, red-shifted fluorophores are still preferred for tissues because of the lower autofluorescence. Figure 4 demonstrates that all ligands bound the Y_1 receptors in a specific manner, but Py5 labelled ligand has more non-specific binding inside cells than other ligands. In addition to usual widefield microscopy, these ligands were also imaged with total internal fluorescence (TIRF) microscopy, which only excites fluorophores that are very close to the coverslip surface, thus reducing background signal and increasing sensitivity. From TIRF studies, the ligand labelled with TAMRA (CM159) is preferred over gadolinium-cyanine (CM139) or Py5 (CM138) due to higher stability and low non-specific binding. However, based on preliminary experiments with brain slices, TAMRA labelled CM159 could not be used in tissues because of the high autofluorescence. In contrast, more red-shifted gadolinium-cyanine labelled CM139 showed promising results.

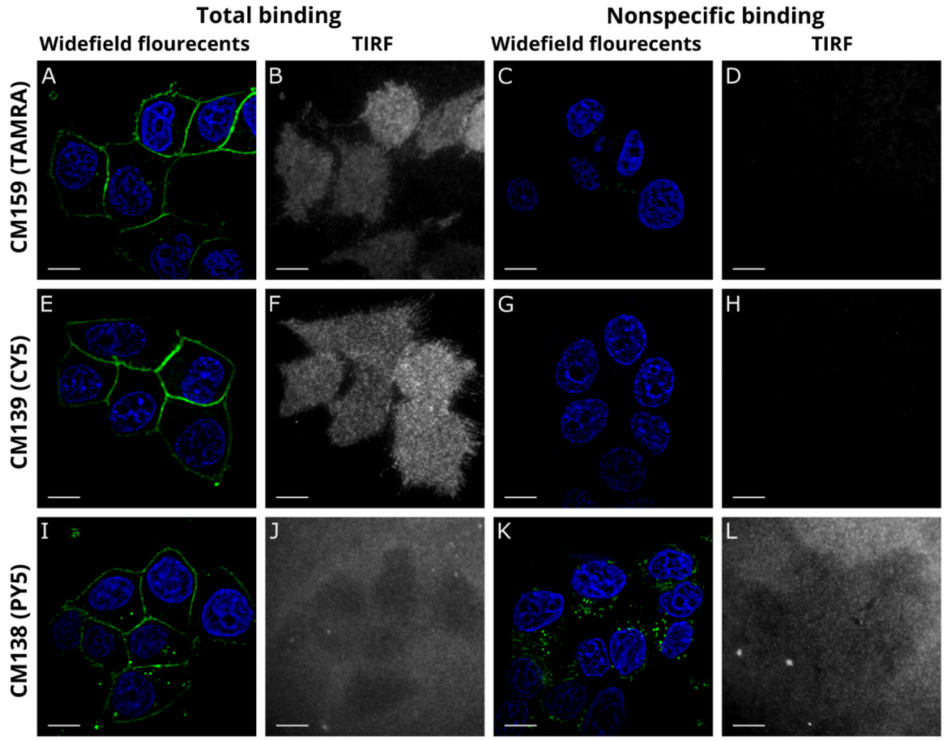

Figure 4 Visualisation of fluorescent ligand binding to MCF-7 breast cancer cells expressing Y_1 receptors using widefield fluorescence and TIRF microscopy. Shown are representative images acquired after incubation of the cells with 1 nM CM159 (A, B), CM139 (E, F), or CM138 (I, J) at 37 °C for (E-H) 30 min or (A-D and I-J) 60 min. Non-specific binding was determined in the presence of 10 μM BIBO3304. The imaging was done as described in **PAPER IV**. The scale bar is 10 μm.

4.5. Implementation of TIRF-based assay for characterization of ligand binding to receptors in BBV

TIRF microscopy also enables ultrasensitive detection of ligand binding to receptors, but in this case, a special assay set-up is required. Therefore in **PAPER V** TIRF microscopy-based assay was developed to measure ligand binding to NPY Y_1 receptors. Because TIRF microscopy only excites the fluorophores close to the coverslip, there is a need to immobilise BBVs to the coverslip. For this application, coverslips were specifically treated to minimise the nonspecific binding. Moreover, specific anchoring molecules were added to specifically immobilise BBV to these coverslips, as depicted in figure 5. Also, a multiwell system was developed to enable HTS. Finally, the amount of bound fluorescent ligand can be assessed by counting spots on TIRF microscopy images, which can be done with the SPOTNIC software. This software was developed and integrated into Aparecium by Tõnis Laasfeld.

This proof of principle study utilised compound 40 (UR-MC026) from **PAPER V**, which is a structural isomer of CM159. The K_d obtained from TIRF microscopy assay system were 100 ± 30 pM and 41 ± 12 pM, depending on whether the fluorescent ligand or receptor concentration was varied. Moreover, the FA assay was used to validate the results obtained from the TIRF microscopy assay, and both K_d values are in good agreement with each other (K_{d_FA} = 120 ± 30 pM). Furthermore, the results from competition binding assays for three unlabeled ligands were also in good agreement for the two assays.

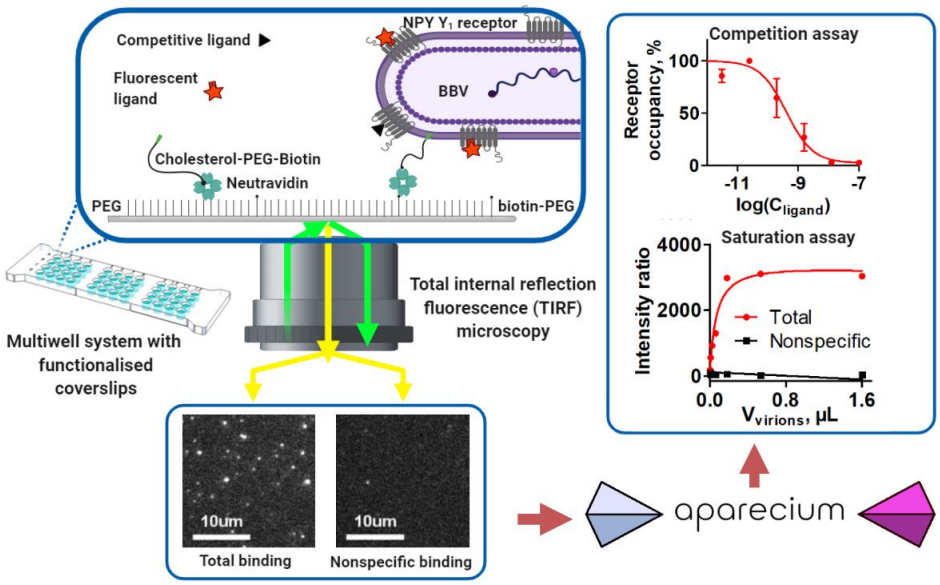

Figure 5 Measurement system set-up for BBVs immobilisation detection and pharmacological characterisation of ligand-receptor interactions with TIRF microscopy. For measurements, the functionalised coverslips were attached to the developed multiwell-system. BBVs as a receptor source are bound to the biotin groups on the coverslip surface with neutravidin and cholesterol-PEG-biotin as an anchor. The ligand binding to receptors was detected with TIRF microscopy as spots in the field of view, quantified with Aparecium toolbox SPOTNIC as a ratio of total spot intensity to the background, and used for pharmacological analysis.

To demonstrate the sensitivity of this assay system, the LoD and LoQ were calculated. Depending on the experiment set-up, if the fluorescent ligand of the receptor concentrations were varied, the LoD was 20 pM or 13 pM, and LoQ was 20 pM or 41 pM. These values for detecting receptor-ligand complex formation were conservative. They can be significantly improved by increasing the number of images from a well and combining measurements from multiple non-specific wells to reduce uncertainty or improve the image analysis algorithm. With these improvements, the measurement system itself may offer sub-picomolar LoD and

LoQ values. Moreover, the LoD and LoQ values are highly dependent on the measured interaction's K_d value, and a higher binding affinity enables lower LoD and LoQ values accordingly. Finally, it must be noted that these LoD and LoQ values do not allow estimating what the LoD and LoQ would be for determining K_d values for other receptor-ligand interactions.

Overall, the TIRF microscopy method is considerably more cumbersome than those discussed above but is of great value for developing test systems for cases where FA is not readily usable. For example, the binding of large protein ligands or ligands with fluorophores that are not applicable to other methods.

4.6. Fluorescent ligand binding detection with FA and Nano-BRET

In addition to NPY fluorescent ligands, Dr Max Keller's workgroup has synthesised fluorescent ligands for Muscarinic acetylcholine receptors. In **PAPER VI**, FA assay and nano-BRET assays were used to characterise two fluorescently labelled ligands, UR-CG072 and UR-MK342, binding to M_2 muscarinic acetylcholine receptors. The big difference between assays is the receptor source. Nano-BRET is conducted with live mammalian cells with modified receptors. In contrast, FA uses BBV with wild-type receptors in insect cell membranes. It is known that the membrane composition of Sf9 cells is different from mammalian cells. Also, the BBV obtained from Sf9 cells lack the components for signal transduction components like G-proteins. However, the nano-BRET assay requires genetic modification of the receptor where the NanoLuc® is generally fused to the N-terminus of the receptor, which may alter the receptor's behaviour. Also, to gather a signal from nano-BRET, the addition of substrate is needed for the assay to function. This limits the measurement length, which can hinder measuring ligands with a slow association or dissociation kinetics.

Both FA and nano-BRET methods were used with two fluorescent ligands to determine ligand binding parameters in **PAPER VI**. Both assays show that UR-CG072 has faster dissociation than UR-MK342. Furthermore, figure 6 shows that UR-MK342 also has a more complicated two-phase dissociation, which complicates the calculation of k_{off}. As this effect is present in both live cells and BBVs, it is connected to the receptor instead of the environment around it. As FA does not have a limit on measurement length like BRET, it was confirmed that UR-MK342 will fully dissociate within 20 h. Overall, the affinities of UR-MK342 obtained from equilibrium binding experiments with both assays are very similar (pK_{d_FA} = 9.30 ± 0.11 pK_{d_BRET} = 9.32 ± 0.16). This confirms that measuring at equilibrium gives still accurate results even if the ligand binding kinetics are more complicated.

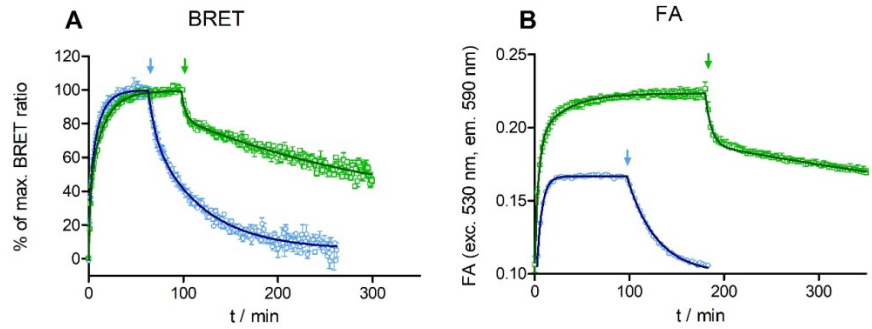

Figure 6 Association and dissociation kinetics of UR-GC072 (blue) and UR-MK342 (green) at the M2 receptor determined in BRET-based (A) and FA-based (B) binding assays. (A) BRET experiments were performed at HEK293T cells, stably expressing the NLuc-M2R. Association was started by adding UR-GC072 and UR-MK342 at a final concentration of 2 nM. Dissociation was initiated after 60 min (1) or 90 min (2) by the addition of an excess of atropine (c_{final} = 2 µM). (B) FA experiments were performed at BBVs displaying the M_2 receptors on the viral envelope. Association was started by the addition of 40 µL baculovirus stock to wells containing UR-GC072 (c_{final} = 2.5 nM) or UR-MK342 (c_{final} = 8 nM). Dissociation was initiated after 95 min (UR-CG072) or 180 min (UR-MK342) by the addition of an excess of atropine (for UR-CG072) or scopolamine (for UR-MK342) (c = 8 µM). The results of individual representative experiments performed in triplicate (BRET) or duplicate (FA) are shown.

UR-CG072 did not have any complicated kinetic patterns, and the determined affinities were also in good agreement (pK_{d_FA} = 9.36 ± 0.02 pK_{d_BRET}= 8.97 ± 0.03). Thus UR-CG072 was a better probe for measuring affinities of unlabelled ligands. The selected unlabelled ligands cover a broad range in affinity values as well as agonists (carbachol, oxotremorine and iperoxo), antagonists (atropine, NMS) and even an allosteric modulator (W84). Generally, affinities of these ligands correlated very well between the FA and nano-BRET assays (R^2 = 0.94) as well as between the FA assay and radioligand binding data (R^2 = 0.94). These results further confirm the relevance of FA assay with BBV as a good method to study ligand binding.

4.7. FA and optical microscopy of live-cells to detect fluorescent ligand binding

Next, in **PAPER VII**, the same ligands were studied with a different muscarinic acetylcholine receptor subtype – the M_4 receptor. The affinities obtained from the radioligand binding assay were in the low nanomolar range (K_i(UR-CG072) = 3.7 ± 0.6 nM; K_i(UR-MK342) = 0.97 ± 0.07 nM (Gruber *et al.* 2020)), which makes them good candidates for probes used FA assay. As expected, the affinities

determined with FA assay for both ligands were in a similar range (K_d(UR-CG072) = 3.6 ± 1.1 nM; K_d(UR-MK342) = 1.2 ± 0.5 nM; table 1). Similarly to the results with M_2 receptors, the dissociation speed of UR-MK342 from M_4 receptors was also slower than UR-CG072. Therefore, UR-CG072 was a better candidate for the live cell assay. Furthermore, regardless of which receptor subtype, M_2 or M_4, is measured, the FA value of the receptor-ligand complex remains the same. This similarity is evident for both fluorescent ligands. In contrast, the receptor-ligand complex FA value depends on the used fluorescent ligand. Also, the FA value is consistently lower for UR-CG072 with both receptor subtypes. These results may indicate that the binding poses and the rotational freedom of the fluorophore moiety are similar between the two subtypes but different for fluorescent ligands. Even if the structure of the ligands is similar, the only variation is in the linker structure that connects the dibenzodiazepinone derivate with the TAMRA fluorophore.

However, both ligands were used in the FA assay to determine the affinities of unlabelled ligands – agonists (acetylcholine, arecoline, pilocarpine, carbachol), antagonists (pirenzepine, atropine, scopolamine, UNSW-MK259, UR-SK59, UR-SK75). Overall, the correlation between affinity values determined with different fluorescent ligands was very high (R^2 = 0.96, Figure 8A).

Table 1. Overview of binding parameters of UR-CG072 and UR-MK342 to M_4 receptor

	Method	K_d (nM) ± S.E.M	k_{on} (nM^{-1} min^{-1}) ± S.E.M	k_{off} (min^{-1}) ± S.E.M
UR-CG072	FA equilibrium	3.6 ± 1.1		
	FA kinetic SB toolbox	8.5 ± 0.8	0.0017 ± 0.0002	0.015 ± 0.002
	Microscopy Saturation	2.85 ± 0.10		
	Microscopy Kinetic	2.6 ± 0.7	0.017 ± 0.007	0.046 ± 0.004
	Radioligand displacement (K_i)	3.7 ± 0.6 (Gruber *et al.* 2020)		
UR-MK342	FA equilibrium	1.2 ± 0.5		
	FA kinetic SB toolbox	1.3 ± 0.4	0.0028 ± 0.0010	0.0037 ± 0.0012
	Radioligand displacement (K_i)	0.97 ± 0.07 (Gruber *et al.* 2020)		

Nano-BRET is closer to the natural system than BBV, but it still needs modified receptors. Thus, in **PAPER VII**, an assay that uses live cells with wild type muscarinic acetylcholine M_4 receptors and the fluorescent ligand UR-GC072 with automated microscopy was developed. A similar assay has been published previously for the dopamine D_3 receptors (Allikalt *et al.* 2021). However, several improvements were made, such as the addition of kinetic measurements of the fluorescent ligand and the usage of convolutional neural networks for image analysis. Also, all the measurements were conducted in the usual cell culture medium with all the additives so that the cells would have as normal an environment as possible. For the new assay, random forest and deep learning-based pipelines for cell segmentation for quantitative image analysis were developed by Tõnis Laasfeld in cooperation with the Department of Computer Science, University of Tartu. The pipelines were integrated into the user-friendly open-source Aparecium software, used throughout the thesis for different data analysis and transformation types. Both image analysis methods were suitable for measuring fluorescence ligand saturation binding and kinetics and screening binding affinities of unlabeled ligands, but the deep learning approach needs fewer images.

The developed live-cell automated microscopy assay can be performed in the saturation binding mode, association, and dissociation kinetic modes and displacement experiments to measure the affinity of unlabelled ligands. The kinetic measurements displayed in Figure 7A show that the fluorescence signal stays relatively stable after the association phase. Moreover, scopolamine induces total displacement of UR-CG072 from the M_4 receptor as the signal reaches the starting value. However, the signal does not reach zero after dissociation, which is caused by autofluorescence, not by incomplete dissociation. UR-CG072 also has sufficiently fast kinetics for performing association and dissociation kinetics. The morphology of CHO-K1-hM_4R cells remains normal, and the cells remain attached to the plate for the entire experiment. Furthermore, Table 1 shows that results obtained with different assays and experimental set-ups are in good agreement.

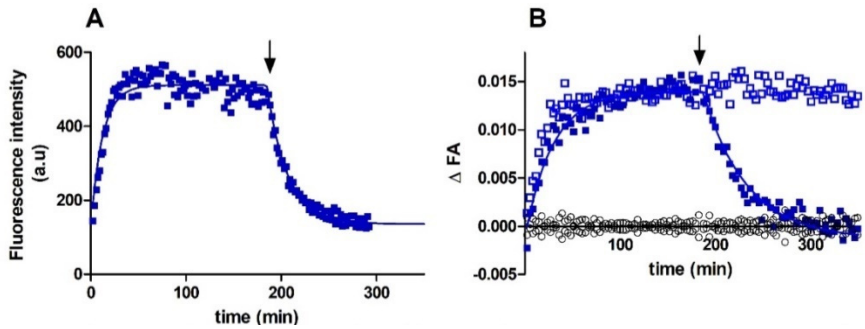

Figure 7 Association and dissociation of UR-CG072 binding to M_4 receptors measured with live-cell microscopy (A) or FA with BBV (B). The arrow indicates the addition of a competitive ligand to start dissociation with 5 µM (A) or 3 µM (B) scopolamine. (A) For live-cell microscopy, the reaction was started by adding 2 nM UR-CG027 to live CHO-K1-hM4R cells. Duplicate values are shown on the graph as separate points to account for the measurement time difference between the replicates. Imaging and image analysis was done as described in **PAPER VII**. (B) FA assay the reaction was initiated by the addition of 20 µL M_4 receptor displaying BBV particles to 5 nM UR-CG072 in the absence (■, □) or presence (○) of 3 µM (B) scopolamine. ΔFA is calculated by subtracting the FA value of non-specific binding from the measured FA value of the corresponding measurement. Representative experiments of at least three independent experiments are shown. The GraphPad Prism model "Association then dissociation" was used for analysis.

Figure 8B shows that pK_i values of M_4 receptor ligands determined with the UR-CG072 using either FA or live-cell microscopy assay were also in good agreement ($R^2 = 0.91$). The live-cell method systematically estimates higher affinities for low-affinity ligands. However, the estimated values are more similar between the assays for high-affinity ligands (Figure 8B). It should be noted that most low-affinity ligands are agonists, while high-affinity ligands are antagonists. Therefore, it is difficult to determine whether there is a systematic difference between assays for low-affinity ligands or simply agonists. Agonism causing the systematic difference is theoretically well-founded, as the high-affinity receptor state is usually stabilised by G-proteins, which are not present in the BBV particles.

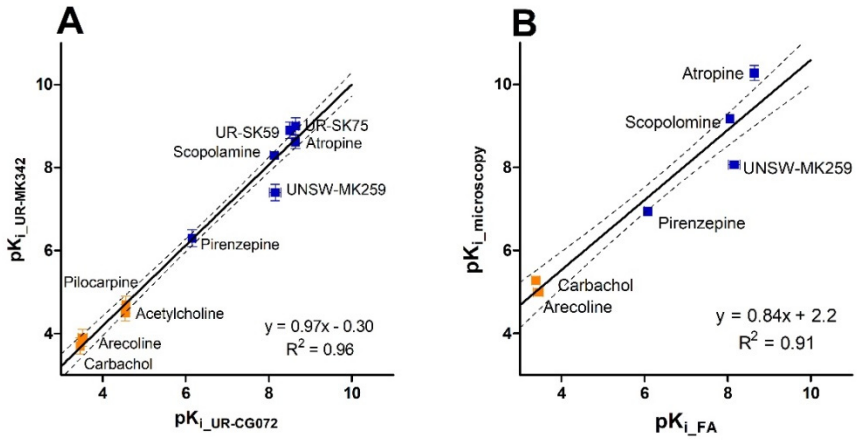

Figure 8 Correlations of binding affinities (pK_i values) of ligands to M_4 receptor, measured with different probes (A) and assays (B). (A) FA assays with UR-CG072 and UR-MK342 were measured after 9 h of incubation. Investigated agonists are presented as orange symbols (■), antagonists as blue symbols (■). Black lines represent linear regression between the datasets, and the dashed black line represents 95%, confidence bands. Data shown for FA and microscopy is the mean of at least three independent experiments, and the error bars represent SEM.

Overall, a similarly good correlation was also found between nanoBRET assay and FA assay using the same probe with M_2 receptor ($R^2 = 0.94$) with the same systematic differences between the pK_i values measured in BBV particles and live cells. This further supports that the systematic difference between the determined agonist pK_i values is caused by differences between BBV particle and live-cell systems.

5. CONCLUSIONS

GPCRs are involved in various vital processes in living organisms, making them an attractive drug target. However, developing better drugs requires better assay systems, enabling to obtain more and higher quality information. This thesis describes the development and application of multiple novel ligand binding assays for GPCRs.

First, to study different receptors from different perspectives, we developed protocols to perform ligand binding experiments to receptors in budded baculoviruses by measuring changes in fluorescence anisotropy. For measurement of activation of receptors, we provided a protocol for determination of intracellular cAMP level using a FRET-based Epac biosensor. Here, we proposed using BacMam gene transfection technology for biosensor expression, which provides higher and more uniform sensor levels in the cells.

Using these methods together, the modulation of the MC_4 receptor by metal ions was demonstrated. FA assay revealed that Cu^{2+} and Zn^{2+} ions inhibit ligand binding to the receptor. In contrast, the response to signal transduction was not as simple. While Zn^{2+} caused MC_4 receptor-dependent activation of the cAMP pathway, Cu^{2+} reduced the activity of MC_4 receptors even below the basal level. Using these two methods together gives a better understanding of the complex modulation of MC_4 receptors.

Using novel NPY Y_1 receptor fluorescent ligands, we showed that they are suitable for characterizing ligand binding to receptors in both BBV and cells. Additionally, we developed TIRF microscopy-based assay system, which allows monitoring ligand binding to individual nanoparticles. This novel assay system gave similar results to the FA assay.

Two novel muscarinic fluorescent ligands were used to determine ligand binding to different receptor subtypes M_2 and M_4 receptors. We compared the FA assay systems to live-cell assay systems. In the case of M_2 receptors, the NanoBRET system is based on the overall fluorescence intensity and can be applied to various cells where expression is high enough. However, NanoBRET uses genetically modified receptors. Therefore, an automated microscopy assay used a machine learning approach for image analysis to measure ligand binding with wild-type M_4 receptors.

In conclusion, the work performed in this thesis is another step in the search for new possibilities for studying G protein-coupled receptors, where the main focus was on the development and validation of the method. These developed assays can now be used in biomedical research to identify the biochemical causes of various diseases and find new selective drugs for a specific target.

REFERENCES

Adan A., Alizada G., Kiraz Y., Baran Y., Nalbant A. (2017) Flow cytometry: basic principles and applications. *Crit. Rev. Biotechnol.* **37**, 163–176.

Allikalt A., Kopanchuk S., Rinken A. (2018) Implementation of fluorescence anisotropy-based assay for the characterization of ligand binding to dopamine D1 receptors. *Eur. J. Pharmacol.* **839**, 40–46.

Allikalt A., Laasfeld T., Ilisson M., Kopanchuk S., Rinken A. (2021) Quantitative analysis of fluorescent ligand binding to dopamine D3 receptors using live-cell microscopy. *FEBS J.* **288**, 1514–1532.

Allikalt A., Rinken A. (2017) Budded baculovirus particles as a source of membrane proteins for radioligand binding assay: The case of dopamine D1 receptor. *J. Pharmacol. Toxicol. Methods* **86**, 81–86.

Bacart J., Corbel C., Jockers R., Bach S., Couturier C. (2008) The BRET technology and its application to screening assays. *Biotechnol. J.* **3**, 311–324.

Bjarnadóttir T. K., Gloriam D. E., Hellstrand S. H., Kristiansson H., Fredriksson R., Schiöth H. B. (2006) Comprehensive repertoire and phylogenetic analysis of the G protein-coupled receptors in human and mouse. *Genomics* **88**, 263–273.

Christopoulos A., Kenakin T. (2002) G Protein-Coupled Receptor Allosterism and Complexing. *Pharmacol. Rev.* **54**, 323–374.

Flanagan C. A. (2016) Chapter 10 – GPCR-radioligand binding assays, in *Methods Cell Biol.*, (K. Shukla A., ed), Vol. 132, pp. 191–215. Academic Press.

Grätz L., Laasfeld T., Allikalt A., Gruber C. G., Pegoli A., Tahk M.-J., Tsernant M.-L., Keller M., Rinken A. (2021) BRET- and fluorescence anisotropy-based assays for real-time monitoring of ligand binding to M2 muscarinic acetylcholine receptors. *Biochim. Biophys. Acta BBA – Mol. Cell Res.* **1868**, 118930.

Gruber C. G., Pegoli A., Müller C., Grätz L., She X., Keller M. (2020) Differently fluorescence-labelled dibenzodiazepinone-type muscarinic acetylcholine receptor ligands with high M_2 R affinity. *RSC Med. Chem.* **11**, 823–832.

Hart H. E., Greenwald E. B. (1979) Scintillation Proximity Assay (SPA)—A new method of immunoassay: Direct and inhibition mode detection with human albumin and rabbit antihuman albumin. *Mol. Immunol.* **16**, 265–267.

Hauser A. S., Attwood M. M., Rask-Andersen M., Schiöth H. B., Gloriam D. E. (2017) Trends in GPCR drug discovery: new agents, targets and indications. *Nat. Rev. Drug Discov.* **16**, 829–842.

Hauser A. S., Avet C., Normand C., Mancini A., Inoue A., Bouvier M., Gloriam D. E. (2022) Common coupling map advances GPCR-G protein selectivity. *eLife* **11**, e74107.

Hilger D., Masureel M., Kobilka B. K. (2018) Structure and dynamics of GPCR signaling complexes. *Nat. Struct. Mol. Biol.* **25**, 4–12.

Jablonski, A (1960) On the notion of emission anisotropy. *Bull. Acad. Pol. Sci*, 259–264.

Jamshad M., Charlton J., Lin Y.-P., Routledge S. J., Bawa Z., Knowles T. J., Overduin M., et al. (2015) G-protein coupled receptor solubilization and purification for biophysical analysis and functional studies, in the total absence of detergent. *Biosci. Rep.* **35**, e00188.

Jean-Charles P.-Y., Kaur S., Shenoy S. K. (2017) GPCR signaling via β-arrestin-dependent mechanisms. *J. Cardiovasc. Pharmacol.* **70**, 142–158.

Jong L. A. A. de, Uges D. R. A., Franke J. P., Bischoff R. (2005) Receptor–ligand binding assays: Technologies and Applications. *J. Chromatogr. B* **829**, 1–25.

Keller M., Bernhardt G., Buschauer A. (2011) [3H]UR-MK136: A Highly Potent and Selective Radioligand for Neuropeptide Y Y1 Receptors. *ChemMedChem* **6**, 1566–1571.

Keller M., Pop N., Hutzler C., Beck-Sickinger A. G., Bernhardt G., Buschauer A. (2008) Guanidine−Acylguanidine Bioisosteric Approach in the Design of Radioligands: Synthesis of a Tritium-Labeled NG-Propionylargininamide ([3H]-UR-MK114) as a Highly Potent and Selective Neuropeptide Y Y1 Receptor Antagonist. *J. Med. Chem.* **51**, 8168–8172.

Keller M., Tränkle C., She X., Pegoli A., Bernhardt G., Buschauer A., Read R. W. (2015a) M2 Subtype preferring dibenzodiazepinone-type muscarinic receptor ligands: Effect of chemical homo-dimerization on orthosteric (and allosteric?) binding. *Bioorg. Med. Chem.* **23**, 3970–3990.

Keller M., Weiss S., Hutzler C., Kuhn K. K., Mollereau C., Dukorn S., Schindler L., Bernhardt G., König B., Buschauer A. (2015b) Nω-Carbamoylation of the Argininamide Moiety: An Avenue to Insurmountable NPY Y1 Receptor Antagonists and a Radiolabeled Selective High-Affinity Molecular Tool ([3H]UR-MK299) with Extended Residence Time. *J. Med. Chem.* **58**, 8834–8849.

King C., Barbiellini B., Moser D., Renugopalakrishnan V. (2012) Exactly soluble model of resonant energy transfer between molecules. *Phys. Rev. B* **85**, 125106.

Klarenbeek J. B., Goedhart J., Hink M. A., Gadella T. W. J., Jalink K. (2011) A mTurquoise-Based cAMP Sensor for Both FLIM and Ratiometric Read-Out Has Improved Dynamic Range. *PLOS ONE* **6**, e19170.

Klarenbeek J., Goedhart J., Batenburg A. van, Groenewald D., Jalink K. (2015) Fourth-Generation Epac-Based FRET Sensors for cAMP Feature Exceptional Brightness, Photostability and Dynamic Range: Characterization of Dedicated Sensors for FLIM, for Ratiometry and with High Affinity. *PLOS ONE* **10**, e0122513.

Kolb P., Kenakin T., Alexander S. P. H., Bermudez M., Bohn L. M., Breinholt C. S., Bouvier M., et al. (2022) Community guidelines for GPCR ligand bias: IUPHAR review 32. *Br. J. Pharmacol.* **n/a**.

Kost T. A., Patrick Condreay J., S. Ames R. (2010) Baculovirus Gene Delivery: A Flexible Assay Development Tool. *Curr. Gene Ther.* **10**, 168–173.

Laasfeld T., Kopanchuk S., Rinken A. (2017) Image-based cell-size estimation for baculovirus quantification. *BioTechniques* **63**.

Langley J. N. (1876) The Action of Pilocarpin on the Sub-Maxillary Gland of the Dog. *J. Anat. Physiol.* **11**, 173–180.

Lee P. H., Miller S. C., Staden C. van, Cromwell E. F. (2008) Development of a Homogeneous High-Throughput Live-Cell G-Protein-Coupled Receptor Binding Assay. *J. Biomol. Screen.* **13**, 748–754.

Lefkowitz R. J. (2004) Historical review: A brief history and personal retrospective of seven-transmembrane receptors. *Trends Pharmacol. Sci.* **25**, 413–422.

Levoye A., Dam J., Ayoub M. A., Guillaume J.-L., Jockers R. (2006) Do orphan G-protein-coupled receptors have ligand-independent functions? New insights from receptor heterodimers. *EMBO Rep.* **7**, 1094–1098.

Ligt R. A. F. de, Kourounakis A. P., IJzerman A. P. (2000) Inverse agonism at G protein-coupled receptors: (patho)physiological relevance and implications for drug discovery. *Br. J. Pharmacol.* **130**, 1–12.

Link R., Veiksina S., Rinken A., Kopanchuk S. (2017) Characterization of ligand binding to melanocortin 4 receptors using fluorescent peptides with improved kinetic properties. *Eur. J. Pharmacol.* **799**, 58–66.

Lohse M. J., Nuber S., Hoffmann C. (2012) Fluorescence/Bioluminescence Resonance Energy Transfer Techniques to Study G-Protein-Coupled Receptor Activation and Signaling. *Pharmacol. Rev.* **64**, 299–336.

Loisel T. P., Ansanay H., St-Onge S., Gay B., Boulanger P., Strosberg A. D., Marullo S., Bouvier M. (1997) Recovery of homogeneous and functional β2-adrenergic receptors from extracellular baculovirus particles. *Nat. Biotechnol.* **15**, 1300–1304.

Makela A. R., Oker-Blom C. (2008) The Baculovirus Display Technology – An Evolving Instrument for Molecular Screening and Drug Delivery. *Comb. Chem. High Throughput Screen.* **11**, 86–98.

Mazina O., Allikalt A., Heinloo A., Reinart-Okugbeni R., Kopanchuk S., Rinken A. (2015) cAMP Assay for GPCR Ligand Characterization: Application of BacMam Expression System, in *G Protein-Coupled Recept. Screen. Assays Methods Protoc.*, (Prazeres D. M. F., Martins S. A. M., eds), pp. 65–77. Springer, New York, NY.

Mazina O., Reinart-Okugbeni R., Kopanchuk S., Rinken A. (2012) BacMam System for FRET-Based cAMP Sensor Expression in Studies of Melanocortin MC1 Receptor Activation. *J. Biomol. Screen.* **17**, 1096–1101.

Mirzadegan T., Benkö G., Filipek S., Palczewski K. (2003) Sequence Analyses of G-Protein-Coupled Receptors: Similarities to Rhodopsin. *Biochemistry* **42**, 2759–2767.

Mou L., Gates A., Mosser V. A., Tobin A., Jackson D. A. (2006) Transient hypoxia induces sequestration of M1 and M2 muscarinic acetylcholine receptors. *J. Neurochem.* **96**, 510–519.

Müller C., Gleixner J., Tahk M.-J., Kopanchuk S., Laasfeld T., Weinhart M., Schollmeyer D., et al. (2022) Structure-Based Design of High-Affinity Fluorescent Probes for the Neuropeptide Y Y1 Receptor. *J. Med. Chem.*

Nelson D. L., Lehninger A. L., Cox M. M. (2008) *Lehninger principles of biochemistry*. Macmillan.

Neubig R. R., Spedding M., Kenakin T., Christopoulos A. (2003) International Union of Pharmacology Committee on Receptor Nomenclature and Drug Classification. XXXVIII. Update on Terms and Symbols in Quantitative Pharmacology. *Pharmacol. Rev.* **55**, 597–606.

Nikolaev V. O., Bünemann M., Hein L., Hannawacker A., Lohse M. J. (2004) Novel Single Chain cAMP Sensors for Receptor-induced Signal Propagation * ♦. *J. Biol. Chem.* **279**, 37215–37218.

Palczewski K., Kumasaka T., Hori T., Behnke C. A., Motoshima H., Fox B. A., Trong I. L., et al. (2000) Crystal Structure of Rhodopsin: A G Protein-Coupled Receptor. *Science* **289**, 739–745.

Paton W. D. M., Rang H. P. (1965) The uptake of atropine and related drugs by intestinal smooth muscle of the guinea-pig in relation to acetylcholine receptors. *Proc. R. Soc. Lond. B Biol. Sci.* **163**, 1–44.

Perrin F. (1929) La fluorescence des solutions – Induction moléculaire. – Polarisation et durée d'émission. – Photochimie. *Ann. Phys.* **10**, 169–275.

Place T. L., Domann F. E., Case A. J. (2017) Limitations of oxygen delivery to cells in culture: An underappreciated problem in basic and translational research. *Free Radic. Biol. Med.* **113**, 311–322.

Rinken A., Lavogina D., Kopanchuk S. (2018) Assays with Detection of Fluorescence Anisotropy: Challenges and Possibilities for Characterizing Ligand Binding to GPCRs. *Trends Pharmacol. Sci.* **39**, 187–199.

Schiöth H. B., Fredriksson R. (2005) The GRAFS classification system of G-protein coupled receptors in comparative perspective. *Gen. Comp. Endocrinol.* **142**, 94–101.

Schmiedeberg O. (1869) *Das Muscarin: das giftige Alkaloid des Fliegenpilzes (Agaricus muscarius L.) : seine Darstellung, chemischen Eigenschaften, physiologischen Wirkungen, toxicologische Bedeutung und sein Verhältniss zur Pilzvergiftung im allgemeinen*. F.C.W. Vogel.

She X., Pegoli A., Mayr J., Hübner H., Bernhardt G., Gmeiner P., Keller M. (2017) Heterodimerization of Dibenzodiazepinone-Type Muscarinic Acetylcholine Receptor Ligands Leads to Increased M2R Affinity and Selectivity. *ACS Omega* **2**, 6741–6754.

Shimada I., Ueda T., Kofuku Y., Eddy M. T., Wüthrich K. (2020) GPCR drug discovery: integrating solution NMR data with crystal and cryo-EM structures, in *NMR Biol. Macromol. Solut.*, pp. 197–220. WORLD SCIENTIFIC.

Sriram K., Insel P. A. (2018) G Protein-Coupled Receptors as Targets for Approved Drugs: How Many Targets and How Many Drugs? *Mol. Pharmacol.* **93**, 251–258.

Stoddart L. A., Kilpatrick L. E., Hill S. J. (2018) NanoBRET Approaches to Study Ligand Binding to GPCRs and RTKs. *Trends Pharmacol. Sci.* **39**, 136–147.

Stoddart L. A., Vernall A. J., Denman J. L., Briddon S. J., Kellam B., Hill S. J. (2012) Fragment Screening at Adenosine-A3 Receptors in Living Cells Using a Fluorescence-Based Binding Assay. *Chem. Biol.* **19**, 1105–1115.

Syrovatkina V., Alegre K. O., Dey R., Huang X.-Y. (2016) Regulation, Signaling and Physiological Functions of G-proteins. *J. Mol. Biol.* **428**, 3850–3868.

Tõntson L., Kopanchuk S., Rinken A. (2014) Characterization of 5-HT1A receptors and their complexes with G-proteins in budded baculovirus particles using fluorescence anisotropy of Bodipy-FL-NAN-190. *Neurochem. Int.* **67**, 32–38.

Veiksina S., Kopanchuk S., Mazina O., Link R., Lille A., Rinken A. (2015) Homogeneous Fluorescence Anisotropy-Based Assay for Characterization of Ligand Binding Dynamics to GPCRs in Budded Baculoviruses: The Case of Cy3B-NDP-α-MSH Binding to MC4 Receptors, in *G Protein-Coupled Recept. Screen. Assays Methods Protoc.*, (Prazeres D. M. F., Martins S. A. M., eds), pp. 37–50. Springer, New York, NY.

Veiksina S., Kopanchuk S., Rinken A. (2010) Fluorescence anisotropy assay for pharmacological characterization of ligand binding dynamics to melanocortin 4 receptors. *Anal. Biochem.* **402**, 32–39.

Veiksina S., Kopanchuk S., Rinken A. (2014) Budded baculoviruses as a tool for a homogeneous fluorescence anisotropy-based assay of ligand binding to G protein-coupled receptors: The case of melanocortin 4 receptors. *Biochim. Biophys. Acta BBA – Biomembr.* **1838**, 372–381.

Wacker D., Stevens R. C., Roth B. L. (2017) How Ligands Illuminate GPCR Molecular Pharmacology. *Cell* **170**, 414–427.

Waller A., Simons P. C., Biggs S. M., Edwards B. S., Prossnitz E. R., Sklar L. A. (2004) Techniques: GPCR assembly, pharmacology and screening by flow cytometry. *Trends Pharmacol. Sci.* **25**, 663–669.

Zhang R., Xie X. (2012) Tools for GPCR drug discovery. *Acta Pharmacol. Sin.* **33**, 372–384.

SUMMARY IN ESTONIAN

Uued fluorestsentsil põhinevad meetodid G-valguga seotud retseptorite transmembraanse signaaliülekande uurimiseks

Rakud võtavad väliskeskkonnas olevat informatsiooni vastu ja annavad edasi membraanis olevate retseptorite kaudu. Lähtudes nende struktuurist ja funktsioneerimise mehhanismidest on retseptorid jagatud kuude erinevasse klassi, millest suurim on G-valk seotud retseptorite klass. Inimese genoomist on tuvastatud ligi 800 erinevat G-valk seotud retseptorit, mis reageerivad väga erinevatele signaalidele, alustades valgusest kuni suurte valkudeni. Samuti on need retseptorid seotud väga erinevate eluks vajalike protsessidega, mistõttu vead retseptorite talitluses on seotud väga erinevate haigustega. Aastal 2017 hinnati, et ligikaudu 35% kõigis Euroopas Liidus ja Ameerika Ühendriikides müügil olevatest retseptiravimitest on sihitud G-valk seotud retseptoritele.

Retseptorite funktsioneerimise mõistmiseks ja uute ravimikandidaatide leidmiseks on oluline teada, kuidas molekulid seostuvad retseptoritega. Algselt teostati katseid loomade, organite või kudedega, kus mõõdeti otsest füsioloogilist vastust lisatud ainele. Radioligandide avastamine muutis võimalikus ligandi ja retseptori interaktsioonide otsese biokeemilise uurimise. Järgmine edasiminek retseptorite uurimises on olnud erinevate fluorestsentsil põhinevate meetodite kasutuselevõtt, mis on loonud palju uusi võimalusi. Käesoleva doktoritöö eesmärk oligi uudsete fluorestsentsil põhinevate katsesüsteemide arendamine ning rakendamine ligandide seostumise uurimiseks erinevatele G-valk seotud retseptoritele.

Kõigepealt koostati ajakohane protokoll ligandi sidumise uurimiseks fluorestsentsanisotroopia meetodiga. Seejuures kasutati retseptorpreparaadina rakkudest pungunud bakuloviiruse. Need on nanoosakesed, mida saadakse putukarakkudest, mida on eelnevalt nakatatud retseptori valku kodeerivate bakuloviirustega. Nakatustsükli käigus transporditakse ekspresseeritud retseptor raku membraanidesse ja järgmise põlvkonna viirus, võtab need rakust pungudes kaasa. Just need pungunud viirused on ka retseptoreid sisaldavad lipiidsed nanoosakesed. Kuna nendes nanoosakestes puuduvad rakusiseseks signaaliülekandeks vajalikud valgud, nagu G-valgud, siis retseptori aktivatsiooni uurimiseks koostati selleks sobiva katsesüsteemi detailne protokoll. See annab detailse juhise, kuidas mõõta elusas rakus sekundaarse virgatsaine cAMP kontsentratsiooni. Selleks kasutatakse geneetiliselt kodeeritud Försteri resonantsenergia ülekandel põhinevat biosensorit, mis sünteesitakse uuritavas rakus, aga mille geneetilise informatsiooni rakkudesse viimiseks kasutatakse viirustel põhinevat BacMam süsteem.

Kombineerides neid kahte meetodit, õnnestus meil näidata Cu^{2+} ja Zn^{2+} ioonide kompleksne mõju melanokortiin 4 retseptori funktsioneerimisele. Mõlemad ioonid takistasid ligandide seostumist retseptorile juba madalal mikromolaarsel kontsentratsioonil. Kuid nad ei toiminud tavaliste inhibiitoritena. Zn^{2+} ioon toimis hoopis aktivaatorina, põhjustades rakusisese cAMP kontsentratsiooni

kasvu, kuid Cu^{2+} oli selgelt inhibiitor, viies cAMP kontsentratsiooni isegi baastasemest madalamale.

Meie koostööpartnerid Regensburgi Ülikoolist (Saksamaa) on sünteesinud mitmeid uudseid fluorestsentsligande, mida me kasutasime neuropeptiid Y ja muskariinsete retseptorite uurimiseks. Uudsed madalmolekulaarsed neuropeptiid Y Y_1 retseptori fluorestsentsligandid omasid pikomolaarset afiinsust ning sobisid hästi bakuloviirustes olevate retseptorite iseloomustamiseks, kuid olid ka efektiivsed elusate rakkude retseptorite märgistamisel. Neid kasutati ka uudse, täielikul sisepeegelduse fluorestsentsmikroskoopial põhineva katsesüsteemi arendamisel, mis võimaldab jälgida ligandide sidumist üksikutele nanoosakestele, mis on immobiliseeritud klaasi pinnale.

Uudseid muskariinsete retseptorite fluorestsentsligande rakendati erinevate muskariinse retseptori alatüüpide iseloomustamiseks. Selle käigus võrreldi fluorestsentsanisotroopia katsesüsteeme elusate rakkudega rakendatavate katsesüsteemidega. M_2 alatüübi puhul kasutati elusates rakkudes NanoBRET süsteemi, mille toimimiseks on vaja fluorestsentsligandi sidumist geneetiliselt muundatud retseptoritele. M_4 alatüübi uurimise käigus, aga arendati välja uus automatiseeritud mikroskoopia katsesüsteem, mis võimaldab määrata ligandi seostumist modifitseerimata retseptoritele elusates rakkudes. Siinjuures rakendati mikroskoopiapiltide analüüsiks erinevaid masinõppe lähenemisi, mis võimaldab kvantifitseerida ligandi seostumist, selle kineetikat ja automatiseerida katsete läbiviimist. Uute katsesüsteemiga saadud tulemused olid heas kooskõlas fluorestsentsanisotroopia tulemustega.

Antud dissertatsioonis saadud tulemused on oluline samm G-valk seotud retseporite uuringutestes, kuna arendatud meetodeid on võimalik rakendada nii retseptorite biokeemiliste mehhanismide uurimisel, kui ka biomeditsiinilistes uuringutes, et leida erinevate haiguste biokeemilisi põhjuseid ning uusi selektiivseid ja konkreetsele märklauale sihitud ravimeid.

ACKNOWLEDGEMENTS

First, I would like to thank all my chemistry teachers, especially Martin Saar, who sparked my interest in biochemistry with the "Elu keemia" course. Next, I would like to thank Professor Ago Rinken for letting me be a member of the GPCR workgroup and for guiding me during my master's and doctoral studies. I am very grateful that You allowed me to learn and teach biochemistry and involved me in many different projects.

Furthermore, I want to express my deepest gratitude to my first supervisor, Dr Olga Kukk (Mazina), for teaching me how to work in a biochemistry laboratory, showing me various tips and tricks and my next supervisor Darja Lavõgina for showing me how efficient a scientist can be. I have learned a lot from both of you and hope to be as good a supervisor and scientist as you.

I would also like to thank all of my former and current colleagues from the Chair of Bioorganic Chemistry. Santa Veikšina and Sergei Kopantšuk for sharing their expert know-how. Many thanks also go to my inspiring student and now co-author Jane Trop for contributing to this work and being so excited about science. Also, all the visiting students, Lukas Grätz, Christoph Müller and Hana Danková, for broadening my horizons. Moreover, a big part of this work was due to the connection made by the COST actions CM1207 GLISTEN and CA18133 ERNEST.

Furthermore, I would like to thank Karin Hellat and all the people in Uurimislabor for giving me the opportunity to practice public speaking and teaching chemistry at many different levels.

Also, I want to thank Anni Allikalt and Mihkel Illison for the long coffee and chocolate breaks and relaxing board game nights. Also, for all the help, inspiration, and guidance along the way.

Last but not least, I would like to thank my and Tõnis's families for all the support during this extra-long school time – Aitäh! Also, I would like to thank Tõnis for always being there with a good joke or a mathematical constant. I could not have done this without you by my side.

"The definition of insanity is doing the same thing over and over and expecting different results."
Albert Einstein

PUBLICATIONS

CURRICULUM VITAE

Name: Maris-Johanna Tahk
Date of birth: June 20, 1994
Citizenship: Estonian
Address: University of Tartu, Institute of Chemistry
Ravila 14a, 50411, Tartu, Estonia
E-mail: maris-johanna.tahk@ut.ee

Education:

2018–…	University of Tartu, PhD student in chemistry
2016–2018	University of Tartu, MSc in chemistry, *cum laude*
2013–2016	University of Tartu, BSc in chemistry
2010–2013	Gustav Adolf Grammar School

Professional employment:

2021–2022	University of Tartu, Institute of Chemistry, Junior Research Fellow (0,5)
2018	Turbliss OÜ, product development specialist (0,25)
2016	University of Tartu, Institute of Chemistry, Chemist

Professional organization:

2017–…	University of Tartu Youth Academy, Investigation Lab instructor
2015–…	Member of the Jury of Estonian Chemistry Olympiad

Scientific publications:

1. Link, R., Veiksina, S., **Tahk, M. J**., Laasfeld, T., Paiste, P., Kopanchuk, S., & Rinken, A. (2020). The constitutive activity of melanocortin-4 receptors in cAMP pathway is allosterically modulated by zinc and copper ions. *Journal of Neurochemistry*, *153*(3), 346–361. https://doi.org/10.1111/jnc.14933
2. Laasfeld, T., Ehrminger, R., **Tahk, M.J**., Veiksina, S., Kolvart, K.R., Min, M., Kopanchuk, S. and Rinken, A. (2021). Budded baculoviruses as a receptor display system to quantify ligand binding with TIRF microscopy. *Nanoscale*, *13*(4), pp.2436–2447. https://doi.org/10.1039/D0NR06737G
3. Grätz, L., Laasfeld, T., Allikalt, A., Gruber, C.G., Pegoli, A., **Tahk, M.J**., Tsernant, M.L., Keller, M. and Rinken, A., (2021). BRET-and fluorescence anisotropy-based assays for real-time monitoring of ligand binding to M2 muscarinic acetylcholine receptors. *Biochimica et Biophysica Acta (BBA)-Molecular Cell Research*, *1868*(3), p.118930. https://doi.org/10.1016/j.bbamcr.2020.118930
4. Veiksina S., **Tahk MJ**., Laasfeld T., Link R., Kopanchuk S., Rinken A. (2021) Fluorescence Anisotropy-Based Assay for Characterization of Ligand Binding Dynamics to GPCRs: The Case of Cy3B-Labeled Ligands Binding to

MC_4 Receptors in Budded Baculoviruses. In: Martins S.A.M., Prazeres D.M.F. (eds) G Protein-Coupled Receptor Screening Assays. Methods in Molecular Biology, vol 2268. Humana, New York, NY. https://doi.org/10.1007/978-1-0716-1221-7_8

5. Lavogina, D., Laasfeld, T., **Tahk, M. J**., Kukk, O., Allikalt, A., Kopanchuk, S., & Rinken, A. (2021). cAMP Biosensor Assay Using BacMam Expression System: Studying the Downstream Signaling of LH/hCG Receptor Activation. In: Martins S.A.M., Prazeres D.M.F. (eds) G Protein-Coupled Receptor Screening Assays. Methods in Molecular Biology, vol 2268. Humana, New York, NY. https://doi.org/10.1007/978-1-0716-1221-7_12
6. Müller, C., Gleixner, J., **Tahk, M.J**., Kopanchuk, S., Laasfeld, T., Weinhart, M., Schollmeyer, D., Betschart, M.U., Lüdeke, S., Koch, P. and Rinken, A., (2022). Structure-Based Design of High-Affinity Fluorescent Probes for the Neuropeptide Y Y1 Receptor. *Journal of Medicinal Chemistry*, *65*(6), pp.4832–4853. https://doi.org/10.1021/acs.jmedchem.1c02033
7. Lavogina D, Lust H, **Tahk M-J,** Laasfeld T, Vellama H, Nasirova N, Vardja M, Eskla K-L, Salumets A, Rinken A, Jaal J. (2022) Revisiting the Resazurin-Based Sensing of Cellular Viability: Widening the Application Horizon. *Biosensors*. 12(4):196. https://doi.org/10.3390/bios12040196
8. **Tahk, M.- J.**, J. Torp, M. A. S. Ali, D. Fishman, L. Parts, L. Grätz, C. Müller, M. Keller, S. Veiksina, T. Laasfeld and A. Rinken (2022). Live-cell microscopy or fluorescence anisotropy with budded baculoviruses – which way to go with measuring ligand binding to M4 muscarinic receptors? *Open Biology, 12*(6), 220019, https://doi.org/10.1098/rsob.220019
9. Ali M.A., Hollo K., Laasfeld T., Torp J., **Tahk M.J.**, Rinken A., Palo K., Parts L., Fishman D. (2022) ArtSeg: Rapid Artifact Segmentation and Removal in Brightfield Cell Microscopy Images. Scientific Reports https://doi.org/10.1038/s41598-022-14703-y6fb25609-0705-4b2b-9758-02e8308f8e8d (In Press)

ELULOOKIRJELDUS

Nimi: Maris-Johanna Tahk
Sünniaeg: 20. juuni 1994
Kodakondsus: Eesti
Aadress: Tartu Ülikool, Keemia instituut
Ravila 14a, 50411, Tartu, Estonia
E-post: maris-johanna.tahk@ut.ee

Haridus:

2018–…	Tartu Ülikool, doktoriõpe keemias
2016–2018	Tartu Ülikool, MSc keemias, *cum laude*
2013–2016	Tartu Ülikool, BSc keemias
2010–2013	Gustav Adolfi gümnaasium

Erialane teenistuskäik:

2020–2021	Tartu Ülikool, Keemia instituut, keemia nooremteadur (0,50)
2018	Turbliss OÜ, tootearenduse spetsialist (0,25)
2016	Tartu Ülikooli Keemia instituut, keemik

Teadusorganisatsioonid:

2017–…	Tartu Ülikooli Teaduskool, loodusteadusliku uurimislabori juhendaja
2015–…	Tartu Ülikooli Teaduskool, keemia olümpiaadi zürii liige

Teaduspublikatsioonid:

1. Link, R., Veiksina, S., **Tahk, M. J**., Laasfeld, T., Paiste, P., Kopanchuk, S., & Rinken, A. (2020). The constitutive activity of melanocortin-4 receptors in cAMP pathway is allosterically modulated by zinc and copper ions. *Journal of Neurochemistry*, *153*(3), 346–361. https://doi.org/10.1111/jnc.14933
2. Laasfeld, T., Ehrminger, R., **Tahk, M.J**., Veiksina, S., Kolvart, K.R., Min, M., Kopanchuk, S. and Rinken, A. (2021). Budded baculoviruses as a receptor display system to quantify ligand binding with TIRF microscopy. *Nanoscale*, *13*(4), pp. 2436–2447. https://doi.org/10.1039/D0NR06737G
3. Grätz, L., Laasfeld, T., Allikalt, A., Gruber, C.G., Pegoli, A., **Tahk, M.J**., Tsernant, M.L., Keller, M. and Rinken, A., (2021). BRET-and fluorescence anisotropy-based assays for real-time monitoring of ligand binding to M2 muscarinic acetylcholine receptors. *Biochimica et Biophysica Acta (BBA)-Molecular Cell Research*, *1868*(3), p. 118930. https://doi.org/10.1016/j.bbamcr.2020.118930
4. Veiksina S., **Tahk MJ**., Laasfeld T., Link R., Kopanchuk S., Rinken A. (2021) Fluorescence Anisotropy-Based Assay for Characterization of Ligand Binding Dynamics to GPCRs: The Case of Cy3B-Labeled Ligands Binding to MC_4 Receptors in Budded Baculoviruses. In: Martins S.A.M., Prazeres

D.M.F. (eds) G Protein-Coupled Receptor Screening Assays. Methods in Molecular Biology, vol 2268. Humana, New York, NY. https://doi.org/10.1007/978-1-0716-1221-7_8

5. Lavogina, D., Laasfeld, T., **Tahk, M. J**., Kukk, O., Allikalt, A., Kopanchuk, S., & Rinken, A. (2021). cAMP Biosensor Assay Using BacMam Expression System: Studying the Downstream Signaling of LH/hCG Receptor Activation. In: Martins S.A.M., Prazeres D.M.F. (eds) G Protein-Coupled Receptor Screening Assays. Methods in Molecular Biology, vol 2268. Humana, New York, NY. https://doi.org/10.1007/978-1-0716-1221-7_12
6. Müller, C., Gleixner, J., **Tahk, M.J**., Kopanchuk, S., Laasfeld, T., Weinhart, M., Schollmeyer, D., Betschart, M.U., Lüdeke, S., Koch, P. and Rinken, A., (2022). Structure-Based Design of High-Affinity Fluorescent Probes for the Neuropeptide Y Y1 Receptor. *Journal of Medicinal Chemistry*, *65*(6), pp. 4832–4853. https://doi.org/10.1021/acs.jmedchem.1c02033
7. Lavogina D, Lust H, **Tahk M-J,** Laasfeld T, Vellama H, Nasirova N, Vardja M, Eskla K-L, Salumets A, Rinken A, Jaal J. (2022) Revisiting the Resazurin-Based Sensing of Cellular Viability: Widening the Application Horizon. *Biosensors*. 12(4):196. https://doi.org/10.3390/bios12040196
8. **Tahk, M.- J.**, J. Torp, M. A. S. Ali, D. Fishman, L. Parts, L. Grätz, C. Müller, M. Keller, S. Veiksina, T. Laasfeld and A. Rinken (2022). Live-cell microscopy or fluorescence anisotropy with budded baculoviruses – which way to go with measuring ligand binding to M4 muscarinic receptors? *Open Biology, 12*(6), 220019, https://doi.org/10.1098/rsob.220019
9. Ali M.A., Hollo K., Laasfeld T., Torp J., **Tahk M.J.**, Rinken A., Palo K., Parts L., Fishman D. (2022) ArtSeg: Rapid Artifact Segmentation and Removal in Brightfield Cell Microscopy Images. Scientific Reports https://doi.org/10.1038/s41598-022-14703-y6fb25609-0705-4b2b-9758-02e8308f8e8d (In Press)

DISSERTATIONES CHIMICAE UNIVERSITATIS TARTUENSIS

1. **Toomas Tamm.** Quantum-chemical simulation of solvent effects. Tartu, 1993, 110 p.
2. **Peeter Burk.** Theoretical study of gas-phase acid-base equilibria. Tartu, 1994, 96 p.
3. **Victor Lobanov.** Quantitative structure-property relationships in large descriptor spaces. Tartu, 1995, 135 p.
4. **Vahur Mäemets.** The ^{17}O and ^{1}H nuclear magnetic resonance study of H_2O in individual solvents and its charged clusters in aqueous solutions of electrolytes. Tartu, 1997, 140 p.
5. **Andrus Metsala.** Microcanonical rate constant in nonequilibrium distribution of vibrational energy and in restricted intramolecular vibrational energy redistribution on the basis of slater's theory of unimolecular reactions. Tartu, 1997, 150 p.
6. **Uko Maran.** Quantum-mechanical study of potential energy surfaces in different environments. Tartu, 1997, 137 p.
7. **Alar Jänes.** Adsorption of organic compounds on antimony, bismuth and cadmium electrodes. Tartu, 1998, 219 p.
8. **Kaido Tammeveski.** Oxygen electroreduction on thin platinum films and the electrochemical detection of superoxide anion. Tartu, 1998, 139 p.
9. **Ivo Leito.** Studies of Brønsted acid-base equilibria in water and non-aqueous media. Tartu, 1998, 101 p.
10. **Jaan Leis.** Conformational dynamics and equilibria in amides. Tartu, 1998, 131 p.
11. **Toonika Rinken.** The modelling of amperometric biosensors based on oxidoreductases. Tartu, 2000, 108 p.
12. **Dmitri Panov.** Partially solvated Grignard reagents. Tartu, 2000, 64 p.
13. **Kaja Orupõld.** Treatment and analysis of phenolic wastewater with microorganisms. Tartu, 2000, 123 p.
14. **Jüri Ivask.** Ion Chromatographic determination of major anions and cations in polar ice core. Tartu, 2000, 85 p.
15. **Lauri Vares.** Stereoselective Synthesis of Tetrahydrofuran and Tetrahydropyran Derivatives by Use of Asymmetric Horner-Wadsworth-Emmons and Ring Closure Reactions. Tartu, 2000, 184 p.
16. **Martin Lepiku.** Kinetic aspects of dopamine D_2 receptor interactions with specific ligands. Tartu, 2000, 81 p.
17. **Katrin Sak.** Some aspects of ligand specificity of P2Y receptors. Tartu, 2000, 106 p.
18. **Vello Pällin.** The role of solvation in the formation of iotsitch complexes. Tartu, 2001, 95 p.
19. **Katrin Kollist.** Interactions between polycyclic aromatic compounds and humic substances. Tartu, 2001, 93 p.

20. **Ivar Koppel.** Quantum chemical study of acidity of strong and superstrong Brønsted acids. Tartu, 2001, 104 p.
21. **Viljar Pihl.** The study of the substituent and solvent effects on the acidity of OH and CH acids. Tartu, 2001, 132 p.
22. **Natalia Palm.** Specification of the minimum, sufficient and significant set of descriptors for general description of solvent effects. Tartu, 2001, 134 p.
23. **Sulev Sild.** QSPR/QSAR approaches for complex molecular systems. Tartu, 2001, 134 p.
24. **Ruslan Petrukhin.** Industrial applications of the quantitative structure-property relationships. Tartu, 2001, 162 p.
25. **Boris V. Rogovoy.** Synthesis of (benzotriazolyl)carboximidamides and their application in relations with *N*- and *S*-nucleophyles. Tartu, 2002, 84 p.
26. **Koit Herodes.** Solvent effects on UV-vis absorption spectra of some solvatochromic substances in binary solvent mixtures: the preferential solvation model. Tartu, 2002, 102 p.
27. **Anti Perkson.** Synthesis and characterisation of nanostructured carbon. Tartu, 2002, 152 p.
28. **Ivari Kaljurand.** Self-consistent acidity scales of neutral and cationic Brønsted acids in acetonitrile and tetrahydrofuran. Tartu, 2003, 108 p.
29. **Karmen Lust.** Adsorption of anions on bismuth single crystal electrodes. Tartu, 2003, 128 p.
30. **Mare Piirsalu.** Substituent, temperature and solvent effects on the alkaline hydrolysis of substituted phenyl and alkyl esters of benzoic acid. Tartu, 2003, 156 p.
31. **Meeri Sassian.** Reactions of partially solvated Grignard reagents. Tartu, 2003, 78 p.
32. **Tarmo Tamm.** Quantum chemical modelling of polypyrrole. Tartu, 2003. 100 p.
33. **Erik Teinemaa.** The environmental fate of the particulate matter and organic pollutants from an oil shale power plant. Tartu, 2003. 102 p.
34. **Jaana Tammiku-Taul.** Quantum chemical study of the properties of Grignard reagents. Tartu, 2003. 120 p.
35. **Andre Lomaka.** Biomedical applications of predictive computational chemistry. Tartu, 2003. 132 p.
36. **Kostyantyn Kirichenko.** Benzotriazole – Mediated Carbon–Carbon Bond Formation. Tartu, 2003. 132 p.
37. **Gunnar Nurk.** Adsorption kinetics of some organic compounds on bismuth single crystal electrodes. Tartu, 2003, 170 p.
38. **Mati Arulepp.** Electrochemical characteristics of porous carbon materials and electrical double layer capacitors. Tartu, 2003, 196 p.
39. **Dan Cornel Fara.** QSPR modeling of complexation and distribution of organic compounds. Tartu, 2004, 126 p.
40. **Riina Mahlapuu.** Signalling of galanin and amyloid precursor protein through adenylate cyclase. Tartu, 2004, 124 p.

41. **Mihkel Kerikmäe.** Some luminescent materials for dosimetric applications and physical research. Tartu, 2004, 143 p.
42. **Jaanus Kruusma.** Determination of some important trace metal ions in human blood. Tartu, 2004, 115 p.
43. **Urmas Johanson.** Investigations of the electrochemical properties of polypyrrole modified electrodes. Tartu, 2004, 91 p.
44. **Kaido Sillar.** Computational study of the acid sites in zeolite ZSM-5. Tartu, 2004, 80 p.
45. **Aldo Oras.** Kinetic aspects of dATPαS interaction with $P2Y_1$ receptor. Tartu, 2004, 75 p.
46. **Erik Mölder.** Measurement of the oxygen mass transfer through the air-water interface. Tartu, 2005, 73 p.
47. **Thomas Thomberg.** The kinetics of electroreduction of peroxodisulfate anion on cadmium (0001) single crystal electrode. Tartu, 2005, 95 p.
48. **Olavi Loog.** Aspects of condensations of carbonyl compounds and their imine analogues. Tartu, 2005, 83 p.
49. **Siim Salmar.** Effect of ultrasound on ester hydrolysis in aqueous ethanol. Tartu, 2006, 73 p.
50. **Ain Uustare.** Modulation of signal transduction of heptahelical receptors by other receptors and G proteins. Tartu, 2006, 121 p.
51. **Sergei Yurchenko.** Determination of some carcinogenic contaminants in food. Tartu, 2006, 143 p.
52. **Kaido Tämm.** QSPR modeling of some properties of organic compounds. Tartu, 2006, 67 p.
53. **Olga Tšubrik.** New methods in the synthesis of multisubstituted hydrazines. Tartu. 2006, 183 p.
54. **Lilli Sooväli.** Spectrophotometric measurements and their uncertainty in chemical analysis and dissociation constant measurements. Tartu, 2006, 125 p.
55. **Eve Koort.** Uncertainty estimation of potentiometrically measured ph and pK_a values. Tartu, 2006, 139 p.
56. **Sergei Kopanchuk.** Regulation of ligand binding to melanocortin receptor subtypes. Tartu, 2006, 119 p.
57. **Silvar Kallip.** Surface structure of some bismuth and antimony single crystal electrodes. Tartu, 2006, 107 p.
58. **Kristjan Saal.** Surface silanization and its application in biomolecule coupling. Tartu, 2006, 77 p.
59. **Tanel Tätte.** High viscosity $Sn(OBu)_4$ oligomeric concentrates and their applications in technology. Tartu, 2006, 91 p.
60. **Dimitar Atanasov Dobchev**. Robust QSAR methods for the prediction of properties from molecular structure. Tartu, 2006, 118 p.
61. **Hannes Hagu**. Impact of ultrasound on hydrophobic interactions in solutions. Tartu, 2007, 81 p.
62. **Rutha Jäger.** Electroreduction of peroxodisulfate anion on bismuth electrodes. Tartu, 2007, 142 p.

63. **Kaido Viht.** Immobilizable bisubstrate-analogue inhibitors of basophilic protein kinases: development and application in biosensors. Tartu, 2007, 88 p.
64. **Eva-Ingrid Rõõm.** Acid-base equilibria in nonpolar media. Tartu, 2007, 156 p.
65. **Sven Tamp.** DFT study of the cesium cation containing complexes relevant to the cesium cation binding by the humic acids. Tartu, 2007, 102 p.
66. **Jaak Nerut.** Electroreduction of hexacyanoferrate(III) anion on Cadmium (0001) single crystal electrode. Tartu, 2007, 180 p.
67. **Lauri Jalukse.** Measurement uncertainty estimation in amperometric dissolved oxygen concentration measurement. Tartu, 2007, 112 p.
68. **Aime Lust.** Charge state of dopants and ordered clusters formation in CaF_2:Mn and CaF_2:Eu luminophors. Tartu, 2007, 100 p.
69. **Iiris Kahn**. Quantitative Structure-Activity Relationships of environmentally relevant properties. Tartu, 2007, 98 p.
70. **Mari Reinik.** Nitrates, nitrites, N-nitrosamines and polycyclic aromatic hydrocarbons in food: analytical methods, occurrence and dietary intake. Tartu, 2007, 172 p.
71. **Heili Kasuk.** Thermodynamic parameters and adsorption kinetics of organic compounds forming the compact adsorption layer at Bi single crystal electrodes. Tartu, 2007, 212 p.
72. **Erki Enkvist.** Synthesis of adenosine-peptide conjugates for biological applications. Tartu, 2007, 114 p.
73. **Svetoslav Hristov Slavov**. Biomedical applications of the QSAR approach. Tartu, 2007, 146 p.
74. **Eneli Härk.** Electroreduction of complex cations on electrochemically polished Bi(*hkl*) single crystal electrodes. Tartu, 2008, 158 p.
75. **Priit Möller.** Electrochemical characteristics of some cathodes for medium temperature solid oxide fuel cells, synthesized by solid state reaction technique. Tartu, 2008, 90 p.
76. **Signe Viggor.** Impact of biochemical parameters of genetically different pseudomonads at the degradation of phenolic compounds. Tartu, 2008, 122 p.
77. **Ave Sarapuu.** Electrochemical reduction of oxygen on quinone-modified carbon electrodes and on thin films of platinum and gold. Tartu, 2008, 134 p.
78. **Agnes Kütt.** Studies of acid-base equilibria in non-aqueous media. Tartu, 2008, 198 p.
79. **Rouvim Kadis.** Evaluation of measurement uncertainty in analytical chemistry: related concepts and some points of misinterpretation. Tartu, 2008, 118 p.
80. **Valter Reedo.** Elaboration of IVB group metal oxide structures and their possible applications. Tartu, 2008, 98 p.
81. **Aleksei Kuznetsov.** Allosteric effects in reactions catalyzed by the cAMP-dependent protein kinase catalytic subunit. Tartu, 2009, 133 p.

82. **Aleksei Bredihhin.** Use of mono- and polyanions in the synthesis of multisubstituted hydrazine derivatives. Tartu, 2009, 105 p.
83. **Anu Ploom.** Quantitative structure-reactivity analysis in organosilicon chemistry. Tartu, 2009, 99 p.
84. **Argo Vonk.** Determination of adenosine A_{2A}- and dopamine D_1 receptor-specific modulation of adenylate cyclase activity in rat striatum. Tartu, 2009, 129 p.
85. **Indrek Kivi.** Synthesis and electrochemical characterization of porous cathode materials for intermediate temperature solid oxide fuel cells. Tartu, 2009, 177 p.
86. **Jaanus Eskusson.** Synthesis and characterisation of diamond-like carbon thin films prepared by pulsed laser deposition method. Tartu, 2009, 117 p.
87. **Marko Lätt.** Carbide derived microporous carbon and electrical double layer capacitors. Tartu, 2009, 107 p.
88. **Vladimir Stepanov.** Slow conformational changes in dopamine transporter interaction with its ligands. Tartu, 2009, 103 p.
89. **Aleksander Trummal.** Computational Study of Structural and Solvent Effects on Acidities of Some Brønsted Acids. Tartu, 2009, 103 p.
90. **Eerold Vellemäe.** Applications of mischmetal in organic synthesis. Tartu, 2009, 93 p.
91. **Sven Parkel.** Ligand binding to 5-HT_{1A} receptors and its regulation by Mg^{2+} and Mn^{2+}. Tartu, 2010, 99 p.
92. **Signe Vahur.** Expanding the possibilities of ATR-FT-IR spectroscopy in determination of inorganic pigments. Tartu, 2010, 184 p.
93. **Tavo Romann**. Preparation and surface modification of bismuth thin film, porous, and microelectrodes. Tartu, 2010, 155 p.
94. **Nadežda Aleksejeva.** Electrocatalytic reduction of oxygen on carbon nanotube-based nanocomposite materials. Tartu, 2010, 147 p.
95. **Marko Kullapere.** Electrochemical properties of glassy carbon, nickel and gold electrodes modified with aryl groups. Tartu, 2010, 233 p.
96. **Liis Siinor.** Adsorption kinetics of ions at Bi single crystal planes from aqueous electrolyte solutions and room-temperature ionic liquids. Tartu, 2010, 101 p.
97. **Angela Vaasa.** Development of fluorescence-based kinetic and binding assays for characterization of protein kinases and their inhibitors. Tartu 2010, 101 p.
98. **Indrek Tulp.** Multivariate analysis of chemical and biological properties. Tartu 2010, 105 p.
99. **Aare Selberg.** Evaluation of environmental quality in Northern Estonia by the analysis of leachate. Tartu 2010, 117 p.
100. **Darja Lavõgina.** Development of protein kinase inhibitors based on adenosine analogue-oligoarginine conjugates. Tartu 2010, 248 p.
101. **Laura Herm.** Biochemistry of dopamine D_2 receptors and its association with motivated behaviour. Tartu 2010, 156 p.

102. **Terje Raudsepp.** Influence of dopant anions on the electrochemical properties of polypyrrole films. Tartu 2010, 112 p.
103. **Margus Marandi.** Electroformation of Polypyrrole Films: *In-situ* AFM and STM Study. Tartu 2011, 116 p.
104. **Kairi Kivirand.** Diamine oxidase-based biosensors: construction and working principles. Tartu, 2011, 140 p.
105. **Anneli Kruve.** Matrix effects in liquid-chromatography electrospray mass-spectrometry. Tartu, 2011, 156 p.
106. **Gary Urb.** Assessment of environmental impact of oil shale fly ash from PF and CFB combustion. Tartu, 2011, 108 p.
107. **Nikita Oskolkov.** A novel strategy for peptide-mediated cellular delivery and induction of endosomal escape. Tartu, 2011, 106 p.
108. **Dana Martin.** The QSPR/QSAR approach for the prediction of properties of fullerene derivatives. Tartu, 2011, 98 p.
109. **Säde Viirlaid.** Novel glutathione analogues and their antioxidant activity. Tartu, 2011, 106 p.
110. **Ülis Sõukand.** Simultaneous adsorption of Cd^{2+}, Ni^{2+}, and Pb^{2+} on peat. Tartu, 2011, 124 p.
111. **Lauri Lipping.** The acidity of strong and superstrong Brønsted acids, an outreach for the "limits of growth": a quantum chemical study. Tartu, 2011, 124 p.
112. **Heisi Kurig.** Electrical double-layer capacitors based on ionic liquids as electrolytes. Tartu, 2011, 146 p.
113. **Marje Kasari.** Bisubstrate luminescent probes, optical sensors and affinity adsorbents for measurement of active protein kinases in biological samples. Tartu, 2012, 126 p.
114. **Kalev Takkis.** Virtual screening of chemical databases for bioactive molecules. Tartu, 2012, 122 p.
115. **Ksenija Kisseljova**. Synthesis of aza-β^3-amino acid containing peptides and kinetic study of their phosphorylation by protein kinase A. Tartu, 2012, 104 p.
116. **Riin Rebane.** Advanced method development strategy for derivatization LC/ESI/MS. Tartu, 2012, 184 p.
117. **Vladislav Ivaništšev.** Double layer structure and adsorption kinetics of ions at metal electrodes in room temperature ionic liquids. Tartu, 2012, 128 p.
118. **Irja Helm.** High accuracy gravimetric Winkler method for determination of dissolved oxygen. Tartu, 2012, 139 p.
119. **Karin Kipper.** Fluoroalcohols as Components of LC-ESI-MS Eluents: Usage and Applications. Tartu, 2012, 164 p.
120. **Arno Ratas.** Energy storage and transfer in dosimetric luminescent materials. Tartu, 2012, 163 p.
121. **Reet Reinart-Okugbeni**. Assay systems for characterisation of subtype-selective binding and functional activity of ligands on dopamine receptors. Tartu, 2012, 159 p.

122. **Lauri Sikk.** Computational study of the Sonogashira cross-coupling reaction. Tartu, 2012, 81 p.
123. **Karita Raudkivi.** Neurochemical studies on inter-individual differences in affect-related behaviour of the laboratory rat. Tartu, 2012, 161 p.
124. **Indrek Saar.** Design of GalR2 subtype specific ligands: their role in depression-like behavior and feeding regulation. Tartu, 2013, 126 p.
125. **Ann Laheäär.** Electrochemical characterization of alkali metal salt based non-aqueous electrolytes for supercapacitors. Tartu, 2013, 127 p.
126. **Kerli Tõnurist.** Influence of electrospun separator materials properties on electrochemical performance of electrical double-layer capacitors. Tartu, 2013, 147 p.
127. **Kaija Põhako-Esko.** Novel organic and inorganic ionogels: preparation and characterization. Tartu, 2013, 124 p.
128. **Ivar Kruusenberg.** Electroreduction of oxygen on carbon nanomaterial-based catalysts. Tartu, 2013, 191 p.
129. **Sander Piiskop.** Kinetic effects of ultrasound in aqueous acetonitrile solutions. Tartu, 2013, 95 p.
130. **Ilona Faustova**. Regulatory role of L-type pyruvate kinase N-terminal domain. Tartu, 2013, 109 p.
131. **Kadi Tamm.** Synthesis and characterization of the micro-mesoporous anode materials and testing of the medium temperature solid oxide fuel cell single cells. Tartu, 2013, 138 p.
132. **Iva Bozhidarova Stoyanova-Slavova.** Validation of QSAR/QSPR for regulatory purposes. Tartu, 2013, 109 p.
133. **Vitali Grozovski**. Adsorption of organic molecules at single crystal electrodes studied by *in situ* STM method. Tartu, 2014, 146 p.
134. **Santa Veikšina**. Development of assay systems for characterisation of ligand binding properties to melanocortin 4 receptors. Tartu, 2014, 151 p.
135. **Jüri Liiv.** PVDF (polyvinylidene difluoride) as material for active element of twisting-ball displays. Tartu, 2014, 111 p.
136. **Kersti Vaarmets.** Electrochemical and physical characterization of pristine and activated molybdenum carbide-derived carbon electrodes for the oxygen electroreduction reaction. Tartu, 2014, 131 p.
137. **Lauri Tõntson**. Regulation of G-protein subtypes by receptors, guanine nucleotides and Mn^{2+}. Tartu, 2014, 105 p.
138. **Aiko Adamson.** Properties of amine-boranes and phosphorus analogues in the gas phase. Tartu, 2014, 78 p.
139. **Elo Kibena**. Electrochemical grafting of glassy carbon, gold, highly oriented pyrolytic graphite and chemical vapour deposition-grown graphene electrodes by diazonium reduction method. Tartu, 2014, 184 p.
140. **Teemu Näykki.** Novel Tools for Water Quality Monitoring – From Field to Laboratory. Tartu, 2014, 202 p.
141. **Karl Kaupmees.** Acidity and basicity in non-aqueous media: importance of solvent properties and purity. Tartu, 2014, 128 p.

142. **Oleg Lebedev**. Hydrazine polyanions: different strategies in the synthesis of heterocycles. Tartu, 2015, 118 p.
143. **Geven Piir.** Environmental risk assessment of chemicals using QSAR methods. Tartu, 2015, 123 p.
144. **Olga Mazina.** Development and application of the biosensor assay for measurements of cyclic adenosine monophosphate in studies of G protein-coupled receptor signalinga. Tartu, 2015, 116 p.
145. **Sandip Ashokrao Kadam.** Anion receptors: synthesis and accurate binding measurements. Tartu, 2015, 116 p.
146. **Indrek Tallo.** Synthesis and characterization of new micro-mesoporous carbide derived carbon materials for high energy and power density electrical double layer capacitors. Tartu, 2015, 148 p.
147. **Heiki Erikson.** Electrochemical reduction of oxygen on nanostructured palladium and gold catalysts. Tartu, 2015, 204 p.
148. **Erik Anderson.** *In situ* Scanning Tunnelling Microscopy studies of the interfacial structure between Bi(111) electrode and a room temperature ionic liquid. Tartu, 2015, 118 p.
149. **Girinath G. Pillai.** Computational Modelling of Diverse Chemical, Biochemical and Biomedical Properties. Tartu, 2015, 140 p.
150. **Piret Pikma.** Interfacial structure and adsorption of organic compounds at Cd(0001) and Sb(111) electrodes from ionic liquid and aqueous electrolytes: an *in situ* STM study. Tartu, 2015, 126 p.
151. **Ganesh babu Manoharan.** Combining chemical and genetic approaches for photoluminescence assays of protein kinases. Tartu, 2016, 126 p.
152. **Carolin Siimenson**. Electrochemical characterization of halide ion adsorption from liquid mixtures at Bi(111) and pyrolytic graphite electrode surface. Tartu, 2016, 110 p.
153. **Asko Laaniste.** Comparison and optimisation of novel mass spectrometry ionisation sources. Tartu, 2016, 156 p.
154. **Hanno Evard.** Estimating limit of detection for mass spectrometric analysis methods. Tartu, 2016, 224 p.
155. **Kadri Ligi.** Characterization and application of protein kinase-responsive organic probes with triplet-singlet energy transfer. Tartu, 2016, 122 p.
156. **Margarita Kagan.** Biosensing penicillins' residues in milk flows. Tartu, 2016, 130 p.
157. **Marie Kriisa.** Development of protein kinase-responsive photoluminescent probes and cellular regulators of protein phosphorylation. Tartu, 2016, 106 p.
158. **Mihkel Vestli.** Ultrasonic spray pyrolysis deposited electrolyte layers for intermediate temperature solid oxide fuel cells. Tartu, 2016, 156 p.
159. **Silver Sepp**. Influence of porosity of the carbide-derived carbon on the properties of the composite electrocatalysts and characteristics of polymer electrolyte fuel cells. Tartu, 2016, 137 p.
160. **Kristjan Haav**. Quantitative relative equilibrium constant measurements in supramolecular chemistry. Tartu, 2017, 158 p.

161. **Anu Teearu**. Development of MALDI-FT-ICR-MS methodology for the analysis of resinous materials. Tartu, 2017, 205 p.
162. **Taavi Ivan**. Bifunctional inhibitors and photoluminescent probes for studies on protein complexes. Tartu, 2017, 140 p.
163. **Maarja-Liisa Oldekop**. Characterization of amino acid derivatization reagents for LC-MS analysis. Tartu, 2017, 147 p.
164. **Kristel Jukk**. Electrochemical reduction of oxygen on platinum- and palladium-based nanocatalysts. Tartu, 2017, 250 p.
165. **Siim Kukk**. Kinetic aspects of interaction between dopamine transporter and *N*-substituted nortropane derivatives. Tartu, 2017, 107 p.
166. **Birgit Viira**. Design and modelling in early drug development in targeting HIV-1 reverse transcriptase and Malaria. Tartu, 2017, 172 p.
167. **Rait Kivi**. Allostery in cAMP dependent protein kinase catalytic subunit. Tartu, 2017, 115 p.
168. **Agnes Heering**. Experimental realization and applications of the unified acidity scale. Tartu, 2017, 123 p.
169. **Delia Juronen**. Biosensing system for the rapid multiplex detection of mastitis-causing pathogens in milk. Tartu, 2018, 85 p.
170. **Hedi Rahnel.** ARC-inhibitors: from reliable biochemical assays to regulators of physiology of cells. Tartu, 2018, 176 p.
171. **Anton Ruzanov.** Computational investigation of the electrical double layer at metal–aqueous solution and metal–ionic liquid interfaces. Tartu, 2018, 129 p.
172. **Katrin Kestav.** Crystal Structure-Guided Development of Bisubstrate-Analogue Inhibitors of Mitotic Protein Kinase Haspin. Tartu, 2018, 166 p.
173. **Mihkel Ilisson.** Synthesis of novel heterocyclic hydrazine derivatives and their conjugates. Tartu, 2018, 101 p.
174. **Anni Allikalt.** Development of assay systems for studying ligand binding to dopamine receptors. Tartu, 2018, 160 p.
175. **Ove Oll.** Electrical double layer structure and energy storage characteristics of ionic liquid based capacitors. Tartu, 2018, 187 p.
176. **Rasmus Palm.** Carbon materials for energy storage applications. Tartu, 2018, 114 p.
177. **Jörgen Metsik.** Preparation and stability of poly(3,4-ethylenedioxythiophene) thin films for transparent electrode applications. Tartu, 2018, 111 p.
178. **Sofja Tšepelevitš.** Experimental studies and modeling of solute-solvent interactions. Tartu, 2018, 109 p.
179. **Märt Lõkov.** Basicity of some nitrogen, phosphorus and carbon bases in acetonitrile. Tartu, 2018, 104 p.
180. **Anton Mastitski**. Preparation of α-aza-amino acid precursors and related compounds by novel methods of reductive one-pot alkylation and direct alkylation. Tartu, 2018, 155 p.
181. **Jürgen Vahter**. Development of bisubstrate inhibitors for protein kinase CK2. Tartu, 2019, 186 p.

182. **Piia Liigand.** Expanding and improving methodology and applications of ionization efficiency measurements. Tartu, 2019, 189 p.
183. **Sigrid Selberg.** Synthesis and properties of lipophilic phosphazene-based indicator molecules. Tartu, 2019, 74 p.
184. **Jaanus Liigand.** Standard substance free quantification for LC/ESI/MS analysis based on the predicted ionization efficiencies. Tartu, 2019, 254 p.
185. **Marek Mooste.** Surface and electrochemical characterisation of aryl film and nanocomposite material modified carbon and metal-based electrodes. Tartu, 2019, 304 p.
186. **Mare Oja.** Experimental investigation and modelling of pH profiles for effective membrane permeability of drug substances. Tartu, 2019, 306 p.
187. **Sajid Hussain.** Electrochemical reduction of oxygen on supported Pt catalysts. Tartu, 2019, 220 p.
188. **Ronald Väli.** Glucose-derived hard carbon electrode materials for sodium-ion batteries. Tartu, 2019, 180 p.
189. **Ester Tee.** Analysis and development of selective synthesis methods of hierarchical micro- and mesoporous carbons. Tartu, 2019, 210 p.
190. **Martin Maide.** Influence of the microstructure and chemical composition of the fuel electrode on the electrochemical performance of reversible solid oxide fuel cell. Tartu, 2020, 144 p.
191. **Edith Viirlaid.** Biosensing Pesticides in Water Samples. Tartu, 2020, 102 p.
192. **Maike Käärik.** Nanoporous carbon: the controlled nanostructure, and structure-property relationships. Tartu, 2020, 162 p.
193. **Artur Gornischeff.** Study of ionization efficiencies for derivatized compounds in LC/ESI/MS and their application for targeted analysis. Tartu, 2020, 124 p.
194. **Reet Link.** Ligand binding, allosteric modulation and constitutive activity of melanocortin-4 receptors. Tartu, 2020, 108 p.
195. **Pilleriin Peets.** Development of instrumental methods for the analysis of textile fibres and dyes. Tartu, 2020, 150 p.
196. **Larisa Ivanova.** Design of active compounds against neurodegenerative diseases. Tartu, 2020, 152 p.
197. **Meelis Härmas.** Impact of activated carbon microstructure and porosity on electrochemical performance of electrical double-layer capacitors. Tartu, 2020, 122 p.
198. **Ruta Hecht.** Novel Eluent Additives for LC-MS Based Bioanalytical Methods. Tartu, 2020, 202 p.
199. **Max Hecht.** Advances in the Development of a Point-of-Care Mass Spectrometer Test. Tartu, 2020, 168 p.
200. **Ida Rahu.** Bromine formation in inorganic bromide/nitrate mixtures and its application for oxidative aromatic bromination. Tartu, 2020, 116 p.
201. **Sander Ratso**. Electrocatalysis of oxygen reduction on non-precious metal catalysts. Tartu, 2020, 371 p.
202. **Astrid Darnell.** Computational design of anion receptors and evaluation of host-guest binding. Tartu, 2021, 150 p.

203. **Ove Korjus.** The development of ceramic fuel electrode for solid oxide cells. Tartu, 2021, 150 p.
204. **Merit Oss.** Ionization efficiency in electrospray ionization source and its relations to compounds' physico-chemical properties. Tartu, 2021, 124 p.
205. **Madis Lüsi**. Electroreduction of oxygen on nanostructured palladium catalysts. Tartu, 2021, 180 p.
206. **Eliise Tammekivi.** Derivatization and quantitative gas-chromatographic analysis of oils. Tartu, 2021, 122 p.
207. **Simona Selberg.** Development of Small-Molecule Regulators of Epi-transcriptomic Processes. Tartu, 2021, 122 p.
208. **Olivier Etebe Nonga.** Inhibitors and photoluminescent probes for in vitro studies on protein kinases PKA and PIM. Tartu, 2021, 189 p.
209. **Riinu Härmas.** The structure and H2 diffusion in porous carbide-derived carbon particles. Tartu, 2022, 123 p.
210. **Maarja Paalo.** Synthesis and characterization of novel carbon electrodes for high power density electrochemical capacitors. Tartu, 2022, 144 p.
211. **Jinfeng Zhao.** Electrochemical characteristics of Bi(hkl) and micro-meso-porous carbon electrodes in ionic liquid based electrolytes. Tartu, 2022, 134 p.
212. **Alar Heinsaar.** Investigation of oxygen electrode materials for high-temperature solid oxide cells in natural conditions. Tartu, 2022, 120 p.
213. **Jaana Lilloja.** Transition metal and nitrogen doped nanocarbon cathode catalysts for anion exchange membrane fuel cells. Tartu, 2022, 202 p.